NEW OBSERVATION OF A HIGHLY AGGRESSIVE DISEASE OF HIBERNATING *MYOTIS LUCIFUGUS* BATS

A Thesis
Submitted to
the Temple University Graduate Board

In Partial Fulfillment
of the Requirements for the Degree
MASTER OF SCIENCE

---

by
Kelly P. Franklin
August 2020

Thesis Approvals:

Brent J. Sewall, Thesis Advisor, Department of Biology

Jocelyn E. Behm, Department of Biology

ABSTRACT

Bats are crucial to ecological function and provide key ecosystem services to people but face a variety of significant threats. One current threat to North American bats is white-nose syndrome (WNS), a disease caused by the invasive fungal pathogen *Pseudogymnoascus destructans* (*Pd*) that has killed millions of hibernating bats across the continent. Remnant populations of affected bat species persist but are so depleted that they may now be highly vulnerable to new threats, or to the synergistic effects of multiple existing threats. The emergence of novel or opportunistic pathogens in bat hosts is a particular concern for the survival of these small, isolated colonies. Apart from studies of WNS and zoonotic pathogens of humans, however, bat diseases remain poorly understood. In this paper, I describe the pathology of a new, highly aggressive bat disease affecting hibernating little brown myotis (*Myotis lucifugus*) and identify candidate microbes as possible causative agents. The pathological signs that were observed diverged from those of WNS, and included blue fluorescence in the wings when trans-illuminated with ultraviolet light, and the rapid development of wing necroses and mortality within weeks of the onset of hibernation. Pathology, wing swab cultures, post-mortem analyses, and hemolysis testing identified an array of candidate species, but suggest that a possible cause is a polymicrobial infection involving two etiological agents – *Trichosporon* yeast and *Serratia* bacteria. Both species have been documented as part of the mycobiota and microbiota of healthy bats, and cave environments. They are also opportunistic pathogens, known to cause infection in other wild animals and immunocompromised humans. Opportunistic pathogens have been increasingly implicated as a cause of mass mortality events in wildlife. The disease identified here has,

to my knowledge, not previously been described, and could represent a new threat to North American bats, compounding concerns for populations facing an already precarious situation.

DEDICATION

This thesis is dedicated to my parents, who have been supportive of my ongoing educational pursuits from art school to graduate school, and every moment in between. Without all of your help and wisdom, I would have never gotten this far – thank you from the bottom of my heart.

ACKNOWLEDGMENTS

I would first like to acknowledge my advisor, Dr. Brent Sewall, for his guidance, immeasurable knowledge, and patience, as I discovered that not all field work goes to plan, and sometimes you have to adapt and move forward with an entirely different idea. I would also like to thank my lab mate, Marianne Gagnon, for all of her help with paperwork, and with fieldwork that required lengthy drives across the state, and for staying awake for a few days in a row to ensure that we got it all done. I appreciate the assistance, wisdom, and kindness that both of these individuals, and all of the Sewall and Freestone labs, have provided me throughout my time at Temple. I would also like to thank Dr. Jocelyn Behm, for serving on my committee and providing insight and advice to help me improve my thesis.

I would like to acknowledge all of hard work of Dr. Barrie Overton and Abigail Rea, who respectively oversaw and assisted in the lab work associated with isolating bacteria and fungi from the bats in this study. Their help and expertise were critical to my understanding of what happened to the bats in this experiment.

I additionally owe a debt of gratitude to Greg Turner and Mike Scafini of the Pennsylvania Game Commission for constructing enclosures, directing capture, and helping to get this study up and running. I also appreciate the help of Dr. Justin Brown, wildlife veterinarian with the Pennsylvania Game Commission, and Dr. Nicole Nemeth, veterinarian with the Southeastern Cooperative Wildlife Disease Study, for examining deceased bats to help me come to conclusions about the cause of death. Also, I owe a big thank you to Stephanie Stronsick, licensed Pennsylvania bat rehabilitator, for allowing me to bring ailing bats by at any hour, and assisting with their recovery. Bats in

Pennsylvania are better off because of these dedicated people who work tirelessly toward their protection and care.

Finally, I have to thank my incredible partner, Zach Prediger, for being my personal chef, occasional chauffer, and the voice of reason throughout this whole process. You've been supportive, kind, and understanding; you've kept me sane, and smiling despite the challenges. Thank you for all of it. I couldn't have asked for a better person – you're the best one.

TABLE OF CONTENTS

Page

ABSTRACT……... ii

DEDICATION……... iv

ACKNOWLEDGMENTS……. v

LIST OF TABLES……. ix

LIST OF FIGURES…… x

CHAPTER

1. NEW OBSERVATION OF A HIGHLY AGGRESSIVE DISEASE OF HIBERNATING *MYOTIS LUCIFUGUS* BATS……...…….…..… 1

1.1 Introduction…… 1

1.2 Methods…….. 4

1.2.1 Ethical statement…….…… 4

1.2.2 Study species and capture site descriptions…… 4

1.2.3 Bat capture and data collection……...… 4

1.2.4 Experimental site description…….. 6

1.2.5 Image analysis…….…… 7

1.2.6 Post-mortem examinations and culturing…….…..…..…….…… 9

1.2.7 Hemolysis testing…….…… 10

1.2.8 Statistical analyses……..…... 11

1.3 Results…….. 13

1.3.1 Field data collection…….……. 13

1.3.1.1 Bats at capture…… 13

1.3.1.2 Signs of WNS infection…… 13

1.3.1.3 Signs of unknown disease…… 13

1.3.1.4 Body condition…… 18

1.3.1.5 Mortality…… 18

1.3.2 Post-mortem examination…… 20

1.3.3 Wing swab samples…… 24

1.3.4 Hemolysis testing…… 25

1.4 Discussion…… 25

1.4.1 Differences between observed disease and WNS…… 27

1.4.2 Host factors associated with disease severity…… 29

1.4.3 Blue fluorescence…… 30

1.4.4 Isolated fungi and bacteria…… 32

1.4.5 Host characteristics influencing disease onset and progression…… 38

1.4.6 Hypothesized disease agents…… 40

1.5 Conclusion…… 41

REFERENCES CITED…… 43

APPENDICES

A. SUPPLEMENTARY METHODS…… 57

B. SUPPLEMENTARY TABLES …… 64

LIST OF TABLES

Table Page

1. Bacteria and fungi isolated from deceased bats provided to Southeastern Cooperative Wildlife Disease Study……... 21

2. Bacteria and fungi isolated from vivisection of one deceased adult bat…….…..…... 22

3. Bacteria and fungi isolated from wing swabs taken from 13 living bats…….…..….. 24

4. Results of hemolysis testing…… 26

B1 Sample sizes throughout the experiment……..…….…..…….……. 64

B2 Percent wing area infected by *Pd* throughout experiment…….…..…….……. 65

LIST OF FIGURES

Figure Page

1. Comparison of progression of the unknown disease (left) and *Pd* wing infection (right) under UV trans-illumination……..……... 8

2. Pathological signs of unknown disease…….…. 14

3. Progression of unknown infection in frequently examined bats……..…...…….…. 15

4. Progression of all non-WNS related wing damage through the first three data collection periods for all bats that had measurements at capture, 2 weeks and 4 weeks ……..……..…… 16

5. Least squares means plot of scaled mass index (SMI) through all data collection periods for all experimental groups……..…..…….. 19

6. *Trichosporon* sp. colonization of adult little brown myotis…… 23

CHAPTER 1

NEW OBSERVATION OF A HIGHLY AGGRESSIVE DISEASE OF HIBERNATING *MYOTIS LUCIFUGUS* BATS

1.1 Introduction

Bats provide many ecosystem services to people, including pest control, seed dispersal, nutrient cycling, and pollination, and are essential to ecological function (Ghanem and Voigt 2012, Kunz et al. 2011). They also face a multitude of threats including disease, disturbance of roosting habitat, loss of foraging areas, pesticide use, climate change, and increased collisions with wind turbines while in flight (Ingersoll et al. 2013). In North America, a particularly dire ongoing threat to hibernating bats is white-nose syndrome (WNS) – a disease first detected at a single site near Albany, New York in 2006 (Blehert et al. 2009) that has since infected 13 North American bat species across 35 of the United States and seven Canadian provinces (WNS Response Team 2020). The causal agent of WNS, *Pseudogymnoascus destructans* (*Pd*), is an invasive fungal pathogen (Lorch et al. 2011, Warnecke et al. 2012), which colonizes the skin of hibernating bats, causing cutaneous lesions in the wing membrane (Blehert et al. 2009), disrupting torpor cycles (Reeder et al. 2012), and leading to dehydration, fat loss, electrolyte imbalance, and mortality (Cryan et al. 2010, Cryan et al. 2013, Verant et al. 2014). Local declines have repeated across so many sites that they have resulted in extensive, regional-scale losses in multiple bat species (Thogmartin et al. 2012, Ingersoll et al. 2016). While the affected species persist across their ranges, many of the remnant colonies have declined so much – often by an order of magnitude or more in little brown

myotis (*Myotis lucifugus*) colonies (Frick et al. 2015) – that the remnant populations could become increasingly susceptible to stochastic variation and other environmental threats (Sun 2016). Further, concurrent threats can act synergistically (Laurance & Useche 2009; Kannan et al. 2010), raising the concern that any new threats could have outsized effects on already compromised populations.

The appearance of new or previously undetected diseases poses a particularly worrisome threat to wildlife (Fey et al. 2015). Discoveries of novel pathogens in a diversity of animal taxa are ongoing globally, with special attention focused on potential invasions that could pose a threat to susceptible host species after introduction (e.g. Blehert et al. 2009, Martel et al. 2014). In some cases, emerging pathogens cause severe harm to host populations already heavily affected by existing infectious diseases or other population stressors (e.g. loss of habitat or environmental contaminants) (Knapp et al. 2016). Another growing concern is opportunistic pathogens, which typically interact with hosts as harmless commensals, but can become pathogenic in certain contexts, such as when triggered by environmental stressors or when provided entrance into the body through a wound or damaged skin (Robinson et al. 2019). In bats, a wide variety of commensal bacteria species are known to be enteropathogens and have the potential to cause opportunistic infections, including *Escherichia coli* and *Salmonella*, *Yersinia*, *Campylobacter, Vibrio*, *Clostridium*, and *Leptospira* species (Mühldorfer 2013). Susceptibility of the host likely depends on intrinsic (e.g., sex, age, reproductive status, social status, body condition, torpor), and extrinsic (e.g., environmental and anthropogenic stressors) factors that may affect immune response, and host resistance or

tolerance to disease (Mühldorfer 2013). Hibernation may be a particularly vulnerable time for bats because torpor is a period of relative immune dormancy (Field et al. 2018).

Despite increasing global concern for diseases in wildlife, research has traditionally focused on studies of bats as actual or potential reservoir hosts for zoonotic outbreaks in human populations (Calisher et al. 2006, Mühldorfer et al. 2011, Chothe et al. 2017), rather than on infectious diseases impacting bats, or the effects of those diseases on the bat hosts (Kunz and Fenton 2003, Lorch et al. 2015). One exception is the recent discovery of a fungal dermatophyte of bats, *Trichophyton redellii*, which is apparently native to North America (Lorch et al. 2015). The fungus, which produced similar clinical signs to WNS, was first documented in Wisconsin, USA at a time when *Pd* invasion appeared imminent, but had not yet occurred there. These circumstances drew the attention of researchers to a disease that would likely have continued to go unnoticed otherwise (Lorch et al. 2015). Thus, potentially harmful pathogens may be affecting bat populations, but remain undetected.

Here, I describe a study that began as an investigation of WNS in captive little brown myotis, hibernating in a semi-natural setting. However, it quickly became apparent that the bats in the experiment were undergoing a different disease entirely – one that caused rapid wing necrosis and mortality during hibernation, prior to any substantial infection by WNS. I then modified the study with the goal of understanding this new, highly aggressive bat disease. Specifically, my objectives were to describe the pathology of the disease and to identify candidate microbes as possible causative agents. In this paper, I explain the progression of this disease, identify opportunistic pathogens as

potential etiological agents, and discuss the implications of my findings for disease ecology and bat conservation.

1.2 Methods

1.2.1 Ethical statement

Ethical approval for vertebrate research was obtained from the Institutional Care and Use Committee of Temple University (protocol 4829 to Dr. Brent J. Sewall). The research was conducted under Scientific Studies Permit 44737 issued by the Pennsylvania Game Commission to Dr. Brent J. Sewall.

1.2.2 Study species and capture site descriptions

For this study, little brown myotis (*Myotis lucifugus*) were challenged with *Pd* with the intent to examine the spread of infection through the hibernation period in as close to natural conditions as possible. Once a common hibernating bat species in Pennsylvania, little brown myotis is one of the species most affected by WNS (Ingersoll et al. 2013). The bats used in this study were captured from a wild maternity colony inhabiting large bat boxes in Huntingdon County, Pennsylvania (for further explanation see Appendix A: Supplementary Methods).

1.2.3 Bat capture and data collection

To reduce the likelihood *Pd* would be present on bats at the onset of the experiment, I avoided capturing bats after their entry into hibernation, since all major hibernacula in Pennsylvania are thought to be contaminated with *Pd* (Sewall et al. 2016). Instead, I focused on bats that had not yet entered hibernation, during the time period after the first bats had already initiated hibernation (bats enter asynchronously over a few-week period in the fall; G. Turner pers. obs.). During this time, *Pd* prevalence and

fungal load are low on bats not yet in hibernation (Langwig et al. 2015). Nine adult and ten juvenile, male little brown myotis were collected from the capture site on October 2, 2018. Upon capture of each bat, a uniquely-numbered, lightweight aluminum band was applied to the right forearm for identification.

At capture and during each data-collection visit to the experimental site, mass (g) and forearm length (mm) were recorded for each bat to establish body condition. From these measurements, scaled mass index (SMI; calculated using the formula (mass [g]*(38.528/forearm length [mm])^3.251)) (Bohonak and Van der Linde 2004, Peig and Green 2009) was calculated. The SMI has stronger theoretical support for use as an indicator of energy reserves for small mammals than a formerly common measure, body mass index (Peig & Green, 2009), and SMI has been gaining increasing acceptance in studies of body condition in bats (Field et al. 2015, Lilley et al. 2016).

In addition to body condition measurements, photos were taken of both wings of each individual bat, trans-illuminated with long-wave (368 nm) ultraviolet light (Turner et al. 2014). UV fluorescence has been adopted as a way to non-destructively examine bats for the presence of *Pd* (McGuire et al. 2016). These images were later analyzed to determine the presence and extent of both WNS and non-WNS infection (see section 1.2.5 Image analysis for more detail). Also, the dorsal side of the right wing of each bat was swabbed five times with one sterile swab, and each swab was placed in an individual sterile tube to be frozen for later laboratory analysis (see section 1.2.6 Post-mortem examinations and culturing for more detail). I followed decontamination protocols (USFWS 2018) to avoid cross-contamination of bats with *Pd* throughout the study (for further explanation of these methods see Appendix A: Supplementary Methods).

1.2.4 Experimental site description

During the experiment, the wild-caught little brown myotis were housed in semi-natural conditions in an abandoned iron mine located in Bucks County, Pennsylvania (hereafter, the experimental site). The mine is long (>1200m), with microclimates suitable for hibernation. In the portion of the experimental site used for this study, during the mid-autumn time period of the study, temperatures averaged 6.9˚C (range: 5.5˚C – 7.8˚C) and relative humidity averaged 92% (range: 81% - 98%). Although the mine formerly served as an important winter hibernaculum (>6400 bats in 2008, mostly little brown myotis), the population plummeted by more than 99% after WNS was discovered there in December 2009. By early 2018, only eight wild bats – including four little brown myotis – hibernated in the entire mine.

In advance of the experiment, four non-adjacent wire-mesh cages were installed in the mine to house the wild-caught little brown myotis in a semi-natural setting. Cages were double-layered to prevent predators from accessing bats. To avoid researcher disturbance of other wild hibernating bats at the site during the study, the cages were installed relatively close to the mine entrance, at locations that maintained stable microclimates and were formerly used by hibernating bats. All cages were placed in the same microclimate, but separated to limit disturbance of bats in other cages while researchers accessed each individual cage. The cages were bolted to the wall of the mine, but open on the wall side to provide bats with access to the mine wall substrate. To challenge bats with *Pd,* I applied inoculated sediment to the cage and mine wall substrate one week prior to the installation of the bats (for further explanation of these methods see Appendix A: Supplementary Methods).

After capture, bats were transported to the experimental site and assigned to one of four study groups, by age (adult, juvenile) and monitoring category (frequently examined, less-examined). Bats were distributed among monitoring categories to maintain roughly equal average body condition between the two juvenile groups, and between the two adult groups. Each of the four groups was placed in a separate cage at the experimental site. One group (less-examined adults) had four individuals, all other groups had five. For the frequently examined groups, data were to be collected at two, four and seven weeks after capture to monitor bat disease progression. For the less-examined groups, data were to be collected only at seven weeks to control for researcher disturbance. Because disease effects were severe in juveniles, however, the last data on juveniles were collected at four weeks post-capture, and the experiment was terminated for those two groups at that time. At the end of the experiment, surviving bats were transferred to a licensed bat rehabilitator for recovery, and deceased bats were collected for post-mortem examination.

1.2.5 Image analysis

To determine the extent of infection, I quantified the percentage of total wing area (both wings combined) with cupping erosions indicative of WNS in all images of bat wings taken under ultraviolet light (368 nm). The erosions, that fluoresce orange-yellow when exposed to ultraviolet light (368 nm), are characteristic of WNS infection (Figure 1F). They were quantified using Image Pro Premiere version 9.3 software (Media Cybernetics), following Turner et al. (2014). After comparison of the location of liquid-filled vesicles and degraded epidermis with areas of fluorescence of the trans-illuminated

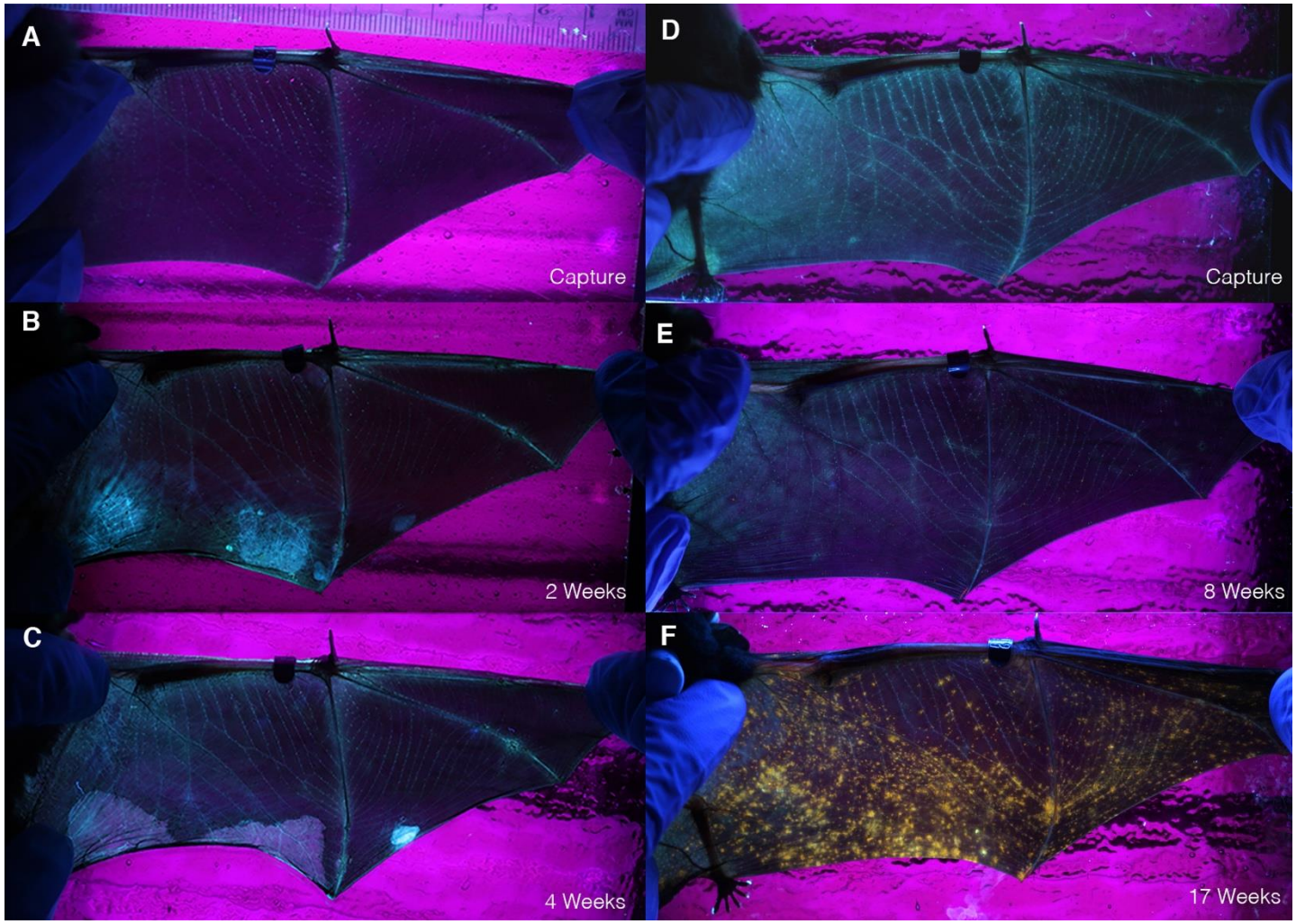

Figure 1. Comparison of the progression of the unknown disease (left) and typical *Pd* wing infection (right) under UV trans-illumination. Adult little brown myotis in this study (left) at (A) capture, (B) 2 weeks and (C) 4 weeks into hibernation. Adult little brown myotis in a different study (right), where bats were experimentally exposed to *Pd* and housed in similar semi-natural conditions, (Gagnon et al. unpublished) at (D) capture, (E) 8 weeks and (F) 17 weeks into hibernation.

bat wings, it became apparent that wing damage was associated with a light blue fluorescence (Figure 1B & 1C). Thus, same images of the bats' wings under UV light were analyzed separately to quantify blue fluorescence and wing damage (Figure 1B & 1C) of any type other than that characteristic of WNS (orange-yellow fluorescence; Figure 1F). Wing damage at the time of capture was minimal at most and, where present, consisted of small pinpoint punctures likely due to flight or mating injuries. These punctures were still counted as wing damage at capture and were included in statistical analyses.

1.2.6 Post-mortem examinations and culturing

Several bats died during the experiment, and to understand the cause of death two distinct post-mortem examinations were employed. First, to narrow the scope of potential causes of death, the seven bats (six juveniles, one adult) that died by week 4 were evaluated by the Southeastern Cooperative Wildlife Disease Study (SCWDS) at the University of Georgia's College of Veterinary Medicine (Athens, GA) via necropsy. Second, the five adult bats found deceased on week 7 were examined, with a focus on isolating specific microbes that could be potential disease-causing agents. This second examination primarily concentrated on one bat from the frequently examined adult group, which appeared to have died just prior to data collection. This bat was dissected to collect skin, liver, heart, and kidney tissues for culture. Liquid-filled vesicles in the wing membrane were observed under a light microscope and samples of the vesicle were cultured. Bacteria and fungi were differentiated using colony and cell morphology and counts on plates. Bacteria were also Gram stained. Individual morphotypes were isolated

and sequenced (for further explanation of these methods see Appendix A: Supplementary Methods).

To obtain more information about the suite of potential disease agents present on the bats, and to clarify the distribution of different microbes across all bats in the study, bacteria and fungi were isolated from swabs taken from the wings of the bats. The last swabs taken from each bat that was alive and measured during at least one data-collection visit (excluding capture) were plated (n=13). These swabs were streaked onto both Acidified Rose Bengal Agar (ARBA) and Tryptic Soy Agar (TSA) media to further examine fungi and bacteria, respectively (for more detailed methods see Appendix A: Supplementary Methods). Microbial colonies of interest were isolated and streaked on individual plates until pure cultures were obtained. For each morphotype, DNA was extracted from individual colonies of bacteria and from scrapings of the mycelium of fungi, and then amplified with PCR so that they could be sequenced (for further explanation of these methods see Appendix A: Supplementary Methods). The sequences obtained were compared to microbial and fungal sequences in NCBI BLAST, GenBank for identification.

1.2.7 Hemolysis testing

Hemolysis testing was used to determine the ability of two potentially pathogenic fungal species isolated from wing swab cultures to lyse red blood cells, a virulence factor for fungi (Aktas and Yigit 2015), relative to *Pd* (isolated from wing swab cultures from a bat in another Pennsylvania study). Six blood agar plates were created on December 12, 2019. To three of the plates, 1mL of 3% dextrose with deionized water was added (Glucose plates). One set of glucose and non-glucose plates was inoculated with each of

three potentially pathogenic organisms of interest: a *Candida* species, and a *Trichosporon* species isolated from wing swab cultures, and *Pd*. The plates were then incubated at 9˚C – 10˚C for 6 days, after which they were observed under a dissecting microscope, and analyzed for hemolysis and sporulation. The plates were returned to incubation for 28 more days, and the observations were repeated. The organisms were then classified by hemolytic activity: Gamma hemolysis (no hemolytic activity), Alpha hemolysis (incomplete hemolysis, expressed as a darkened halo around the underside of the fungal colony), or Beta hemolysis (complete hemolysis, expressed as a clear region around the fungal colony).

1.2.8 Statistical analyses

Several analyses were conducted to evaluate variation in disease effects. Factors influencing WNS infection among bats in the experiment were not statistically assessed, since WNS infection was negligible by the end of the experiment (see Results). Instead, the focus was on evaluating how body condition (SMI) and non-WNS wing damage varied by age (juveniles versus adults), monitoring category (frequently examined versus less-examined), and data collection period. Not all data could be included in single comprehensive analyses because timing of sampling sometimes differed among groups; not all groups were measured in every data collection period due to the sampling design, increasing mortality, and the need to end the experiment early for juveniles (Supplementary Table B1). Therefore, analyses were limited to cases where comparable subsets of the data were available.

For instance, two separate analyses of body condition were conducted, one in frequently examined groups only, and one in juveniles only. Global ANOVA models,

with the SMI as the response, had fixed effects of either age (in the analysis of frequently examined groups), or disturbance (in the analysis of juveniles), data collection period (capture, week 2, week 4, week 7), as well as their interaction. A random effect of the bat band number was used to account for repeated measures of the same individuals over time. Model selection was determined by the small-sample-size-corrected version of Akaike's Information Criterion (AICc), and, in both cases, the sole model with substantial support had only one fixed effect: data collection period. Samples were then pooled by age and monitoring category, and the full dataset was used to analyze an SMI model with a fixed effect of data collection period, and a random effect of bat individual.

For wing damage, because of the sampling design, increasing mortality over time, and the need for early termination of the juvenile experiment, data were sufficient for analysis only in the frequently examined groups, and only at capture and the first two data collection periods (week 2, week 4). The small sample size necessitated a simple model, and an ANOVA with a response of the natural logarithm of wing damage after the addition of 0.01 (half of the minimum non-zero value), a single fixed effect of data collection period, and a repeated measures block by bat individual was employed.

Shapiro-Wilk tests were conducted to verify normality of data, as well as Levene's tests to establish homogeneity of variance between data sets. Tukey HSD tests were used to evaluate differences among groups. An alpha level of 0.5, and one-tailed tests were used to examine predictions that SMI would decrease over time, and that wing damage would increase. Analyses were conducted in JMP statistical software (SAS 2018) and figures generated in R (R Core Team 2018).

1.3 Results

1.3.1 Field data collection

1.3.1.1 Bats at capture

The SMI did not vary among the four groups at capture (ANOVA, $p = 0.185$). One juvenile displayed minimal signs of WNS infection at capture (< 0.1% of wing area with characteristic fluorescence of WNS under UV trans-illumination), and there were no superficial signs of wing damage associated with the spots (Supplementary Table B2).

1.3.1.2 Signs of WNS infection

No bats ever exhibited *Pd* infection in greater than 0.1% of their total wing area (left and right wings combined), including the juvenile that displayed fluorescent lesions at capture (Supplementary Table B2). Fluorescent lesions indicative of *Pd* appeared infrequently in the bats and did not spread much through the duration of the experiment.

1.3.1.3 Signs of unknown disease

As I photographed the wings of the bats on week 2, it became apparent that a non-WNS infection was occurring in both the adult and juvenile bats. The typical progression of this infection began with the appearance of blue fluorescent vesicles in the wings (Figure 2, red circles) or blue fluorescent areas of the wing (Figure 2, arrowheads), continued with the deterioration of melanized skin, and resulted in clear connective tissue being exposed (Figure 3C & 3E, black arrows). The tissue would then tear, or dry out and flake off, culminating in large holes or gaps in the wing membrane (Figure 3E & 3F, white arrows). Wing damage increased steadily throughout the duration of this experiment (ANOVA; model $R^2 = 0.815$, period, $F_{2, 10} = 7.46$, $p = 0.005$; Figure 4).

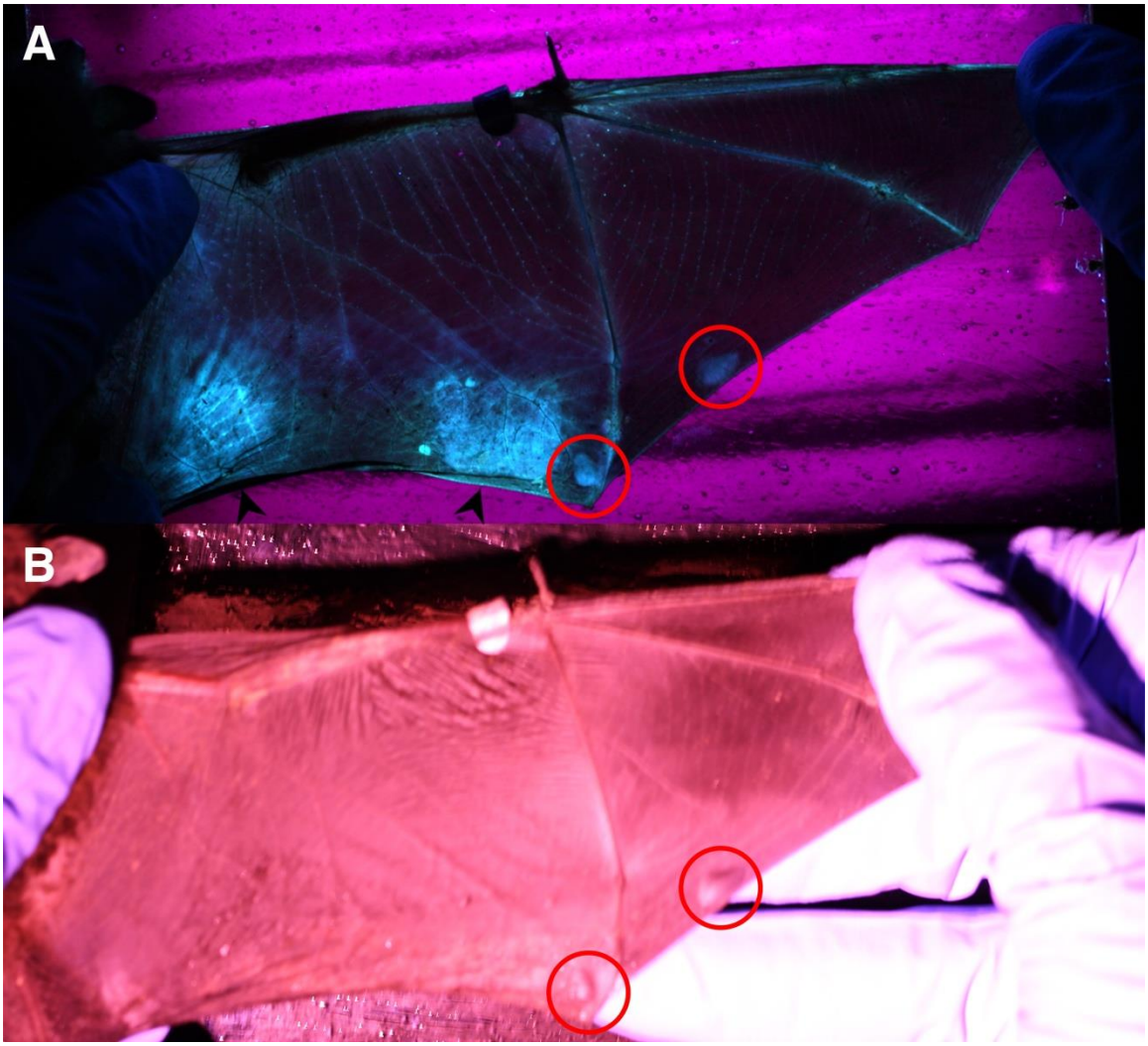

Figure 2. Pathological signs of unknown disease. Pathological signs of infection include wing vesicles (circled in red) that develop prior to the loss of melanized skin from the area. (A) The vesicles fluoresce blue when trans-illuminated with UV light (368 nm). (B) Illuminating the wing with a headlamp shows the dimension of the same wing vesicles. Arrowheads in (A) point to areas where the ventral (opposite the camera) layer of the epidermis has been destroyed, allowing for blue fluorescence of the connective tissue. Bat pictured is the same individual in the top three panels of Figure 3.

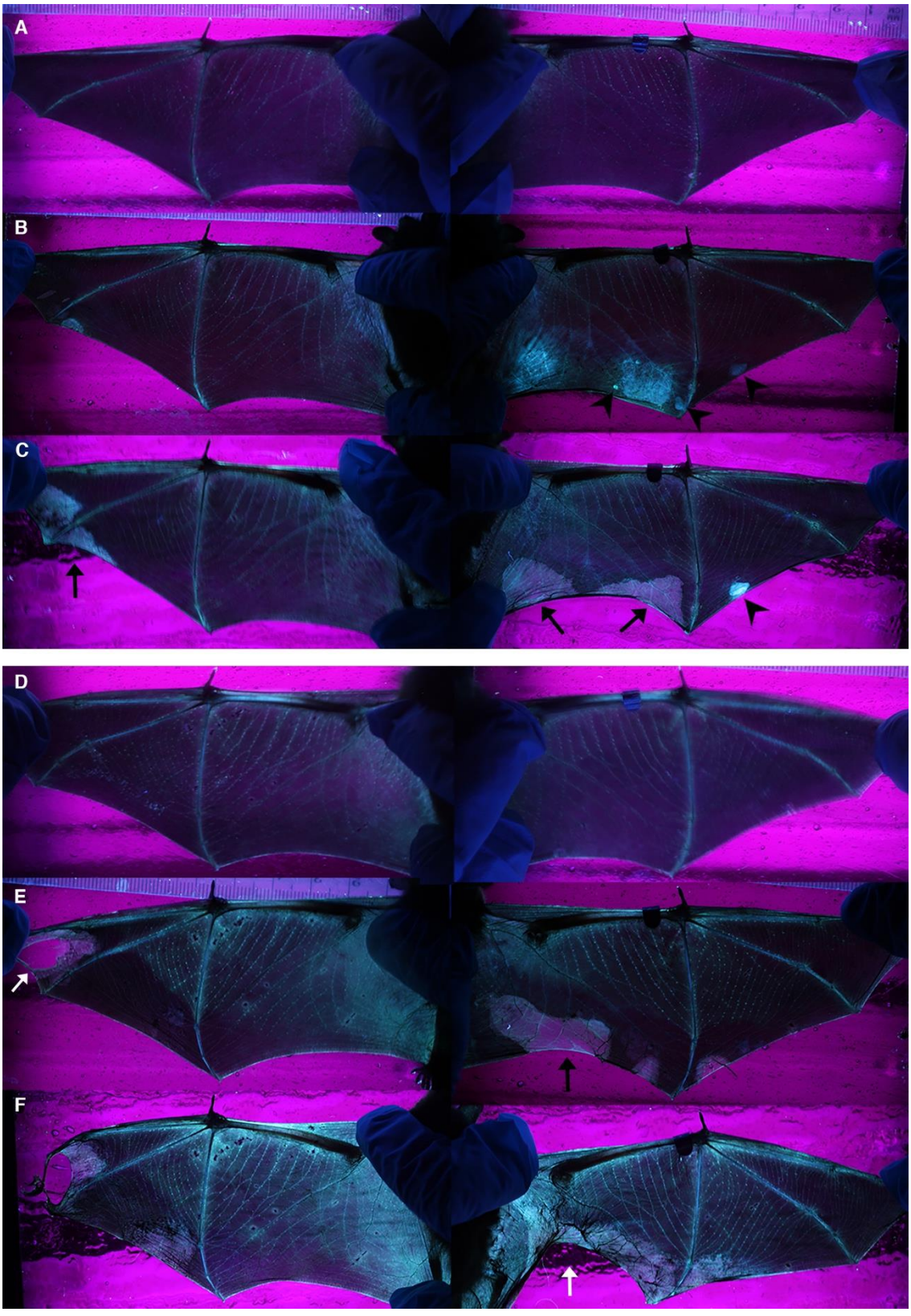
A
B
C
D
E
F

Figure 3. Progression of unknown infection in frequently examined bats. Progression of wing damage associated with the unknown disease in a juvenile (top three panels) little brown myotis from (A) capture, (B) 2 weeks and (C) 4 weeks into the experiment. Progression of wing damage associated with the unknown disease in an adult (bottom three panels) little brown myotis from (D) capture, (E) 2 weeks and (F) 4 weeks into the experiment. Arrowheads point to fluid-filled vesicles in the wing. Black arrows point to sticky, clear connective tissue, seen after the epidermis disappears. White arrows point to wing holes that result from connective tissue tearing, or drying and flaking off. The bat in the top three panels was alive for all three photographs; the bat in the bottom three panels was alive in the first two photographs, but deceased in (F).

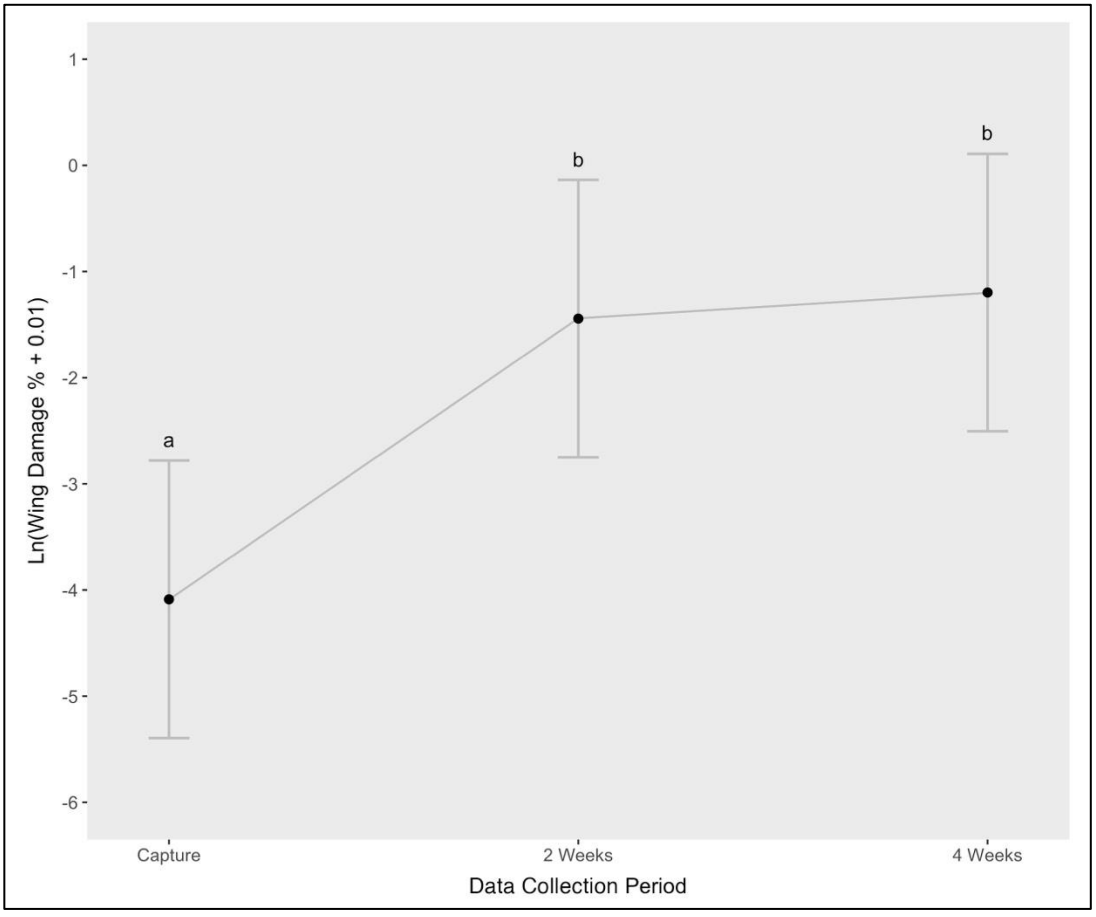

Figure 4. Progression of all non-WNS related wing damage through the first three data-collection periods for all bats that had measurements at capture, 2 weeks and 4 weeks. Periods sharing the same letter are not significantly different from each other. Whiskers indicate 95% upper and lower confidence limits.

By week 2, three of the five adults in the frequently examined group (60% of the group), as well as four of the five juveniles in the frequently examined group (80% of the group) displayed signs of wing damage related to the non-WNS infection. Data was not collected for the two less-examined groups on week 2.

By week 4, six of the ten total juveniles (60%) displayed wing damage. Only two of the five frequently examined juveniles survived to week 4, and both showed signs of wing damage at that point. The top three panels of Figure 3 show the progression of wing damage in one of the two surviving frequently examined juveniles. Some areas of the wing where vesicles had been seen on week 2 (Figure 3B, arrowheads) were either missing entirely, or connected by only thin, clear membranes and elastin strands by week 4 (Figure 3C, black arrows). There were only two surviving juveniles in the less-examined group by week 4, neither of which showed signs of wing damage. In the frequently examined group of adults, three of the five adults (60% of the group) continued to display wing damage; the damage had intensified since week 2. The other two did not exhibit any signs of wing damage. One of the three with wing damage was found deceased on week 4. The bottom three panels of Figure 3 show the progression of wing damage in the frequently examined adult that was found deceased on week 4. In areas where elastin had already been exposed (Figure 3E, black arrows), large holes and gaps in the wing developed by week 4 (Figure 3F, white arrows). Of the nine total adults that started the experiment, eight showed signs of wing damage (88.9%) by week 7.

Among surviving bats transferred to the bat rehabilitator, similar signs continued during supportive care in euthermy. Skin necroses were also exhibited on other exposed

skin surfaces during rehabilitation, and extended beyond the wing membranes to also include the muzzle, ears, tail membrane, and feet (S. Stronsick, pers. obs.).

1.3.1.4 Body condition

Body condition, measured as scaled mass index (SMI), also deteriorated rapidly from the onset of hibernation and continued to deteriorate through the end of the experiment (ANOVA; model $R^2 = 0.985$, period, $F_{2, 17.02} = 330.36$, $p < 0.0001$; Figure 5). The relationship between SMI at capture and date of death was not significant for either the adult (linear regression, $p = 0.079$) or juvenile groups ($p = 0.075$).

1.3.1.5 Mortality

On week 2, all ten bats in the frequently examined groups were alive (the less-examined groups were not observed). Thereafter, juvenile bats died at a faster rate than the adults. By week 4, six of the ten juveniles (60%) had died. The experiment was terminated for juveniles, and the four surviving juveniles that were transferred to the rehabilitator died by mid-December 2018. In contrast, there was one death among five in the frequently examined adult group (20%) by week 4 of the experiment. By week 7, six of the nine adult bats died in total (66.7%). The experiment was then terminated completely, and the three surviving adults were taken to the rehabilitator. Two of these three adults survived in rehabilitation; the third one died in January 2019.

Overall, mortality was high. Of the 19 bats that entered the experiment, only seven (four juveniles, three adults; 36.8%) survived to be taken to rehabilitation. And despite attempts by rehabilitators to combat the infection, disease signs continued and

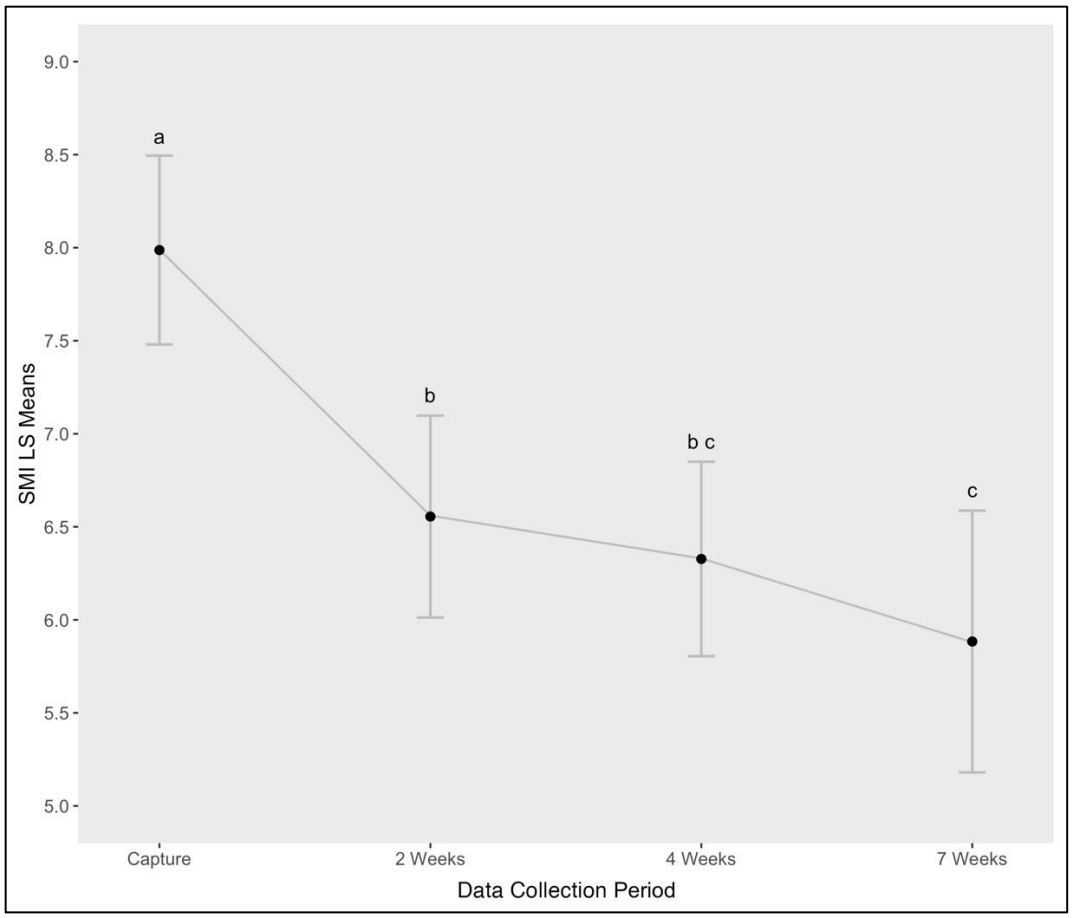

Figure 5. Least squares means plot of the scaled mass index (SMI) through all data collection periods for all experimental groups. Periods sharing the same letter are not significantly different from each other. Whiskers indicate 95% upper and lower confidence limits.

ultimately only two (both adults) of the five bats in rehabilitation survived – a much lower rate than is typical at the same rehabilitation center (S. Stronsick, pers. obs.); these deaths were all attributed directly to the disease. In total, 17 of the 19 bats that started the experiment (89.5%) died as a result of the unidentified disease.

1.3.2 Post-mortem examination

The seven deceased bats from the first mortality event were necropsied by pathologists at SCWDS. Observed pathological signs included severe thinning of the wing membrane, subcutaneous patagial inflammation and edema (clear sections) of the wing, and expanded collagen fibers in the bats' wings. Hemorrhage occurred over areas of edema. In several sections of wings, neutrophils were scattered, and occasionally aggregated, throughout the dermis. Several bats were found to have rare superficial fungi on the skin surface and within the dermis. Fungal elements and hyphae elevated the epidermis in focused areas. Multiple clusters of aggregated yeast cells were found within the keratin layers of the wings and scattered throughout the parenchyma. Large, mixed bacterial colonies, predominately consisting of short bacilli, were found within the dermis and blood vessels. In most instances there were no signs of corresponding cellular reaction, so these colonies were considered to be postmortem overgrowth. Internally, there was hemorrhage or degeneration in the hearts, brains, lungs, intestines, and kidneys of the bats. Several of the bats also had mild parasite loads, including intestinal trematode infection and renal coccidiosis, neither of which are likely to be significant causes of mortality. Bacilli colonies were found in the lumen of the intestinal tract, in blood vessels and throughout the epicardium of the heart, and in blood vessels and sinusoids of the liver in several bats. In their examination, pathologists cultured bacteria and fungi from pooled samples of wings from three bats, and the heart and liver of two other individual bats (Table 1). The species identity of observed yeasts was not determined.

From the bat that was discovered deceased on week 7 and was examined in detail at Lock Haven University, five bacterial species were isolated (Table 2). The most

ubiquitous bacterial species isolated was *Serratia liquefaciens*, which was isolated from the liver, lung, heart, and kidney, but not seen on the wing culture. The single fungal species isolated was a yeast – a *Trichosporon* species. *Trichosporon* was isolated from the wings, but colonized the skin of the ear, and muzzle as well (Figure 6). GenBank accession numbers and percentages of genetic identification are presented along with the species and origin of isolate (Table 2).

Domain/ Kingdom	Species	Gram + / -	Origin of Isolate		
			Wing	Heart	Liver
Bacteria	*Carnobacterium maltaromaticum*	+	✓	✓	
Bacteria	*Hafnia alvei*	-	✓		✓
Bacteria	*Lactococcus raffinolactis*	+			✓
Fungi	*Mucor saturninus*		✓		
Bacteria	*Obseumbacterium proteus*	-	✓		
Fungi	*Penicillium sp.*		✓		

Table 1. Bacteria and fungi isolated from deceased bats provided to Southeastern Cooperative Wildlife Disease Study Microbes listed were found in at least one of the seven bats necropsied.

Domain / Kingdom	Species	Gram + / -	Origin of Isolate					% Identification	Accession no.
			Wing	Liver	Lung	Heart	Kidney		
Bacteria	*Carnobacterium maltaromaticum*	+					✓	99.86%	MH119758
Bacteria	*Flavobacterium sp.*	-	✓					94.48%	MH019224
Bacteria	*Pseudomonas brenneri*	-	✓		✓	✓		100%	KY939742
Bacteria	*Serratia liquefaciens*	-		✓	✓	✓	✓	99.89%	MH190215
Fungi	*Trichosporon sp.*		✓					99.79%	JX270347

Table 2. Bacteria and fungi isolated from vivisection of one deceased adult little brown myotis GenBank accession numbers and percentages of genetic identification are presented, along with the species and origin of isolate.

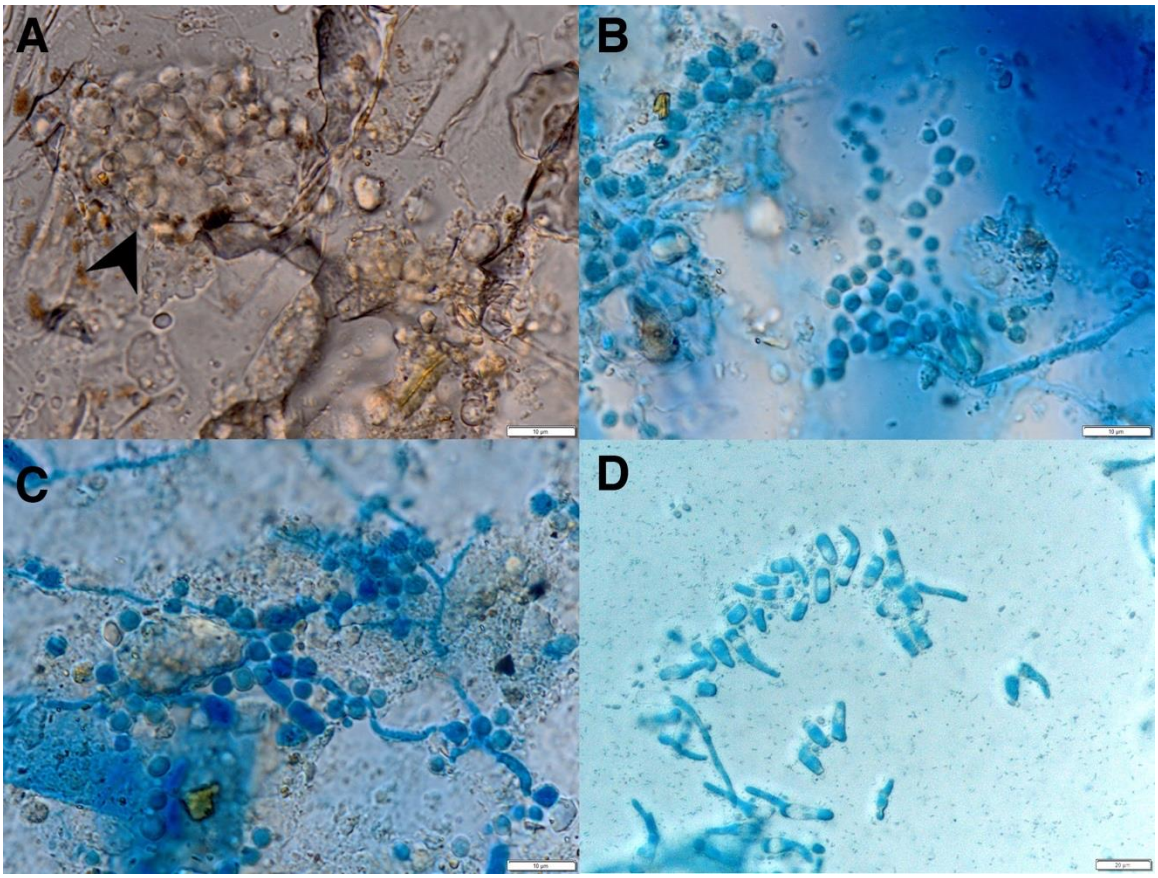

Figure 6. *Trichosporon* sp. colonization of adult little brown myotis. *Trichosporon* sp. colonized the (A) wing, (B) muzzle, and (C) ear of an adult little brown myotis from the frequently examined group. (A) Arrowhead points to aggregated *Trichosporon* yeast cells with a vesicle in the epidermis of the wing. (D) *Trichosporon* sp. isolated in pure culture. Scale bars for (A), (B), (C), are 10µm, and for (D) is 20µm.

1.3.3 Wing swab samples

Cultures obtained from the last swabs taken from the wings of 13 living bats represented all of the age and monitoring categories. Eight bacterial species and two yeasts were identified from these swabs (Table 3). Other saprotrophic fungi common to cave environments were excluded from sequencing but identified from culture as *Penicillium* species, *Cladosporium* species, and *Mucor* species. GenBank accession numbers and identification percentages are presented in Table 3 with the species discovered from wing swab analyses.

Domain / Kingdom	Species	Gram + / -	No. of Isolates	% Identification	Accession no.
Bacteria	*Acinetobacter sp.*	-	1	99.76%	KX989441
Bacteria	*Arthrobacter antarcticus*	+	1	100%	KF318385
Fungi	*Candida glaebosa*		1	98.59%	KX859656
Bacteria	*Pseudomonas fluorescens*	-	1	99.35%	MN334237
Bacteria	*Pseudomonas gessardii*	-	2	100%	MN685265
Bacteria	*Pseudomonas sp.*	-	1	100%	MK373728
Bacteria	*Pseudomonas sp.*	-	1	99.93%	KR054988
Fungi	*Rhodotorula mucilaginosa*		3	100%	MG009546
Bacteria	*Serratia sp.*	-	1	100%	KY780231
Bacteria	*Staphylococcus sciuri*	+	2	100%	CP041879
Bacteria	*Staphylococcus stepanovicii*	+	2	100%	MF678911

Table 3. Bacteria and fungi isolated from wing swabs taken from 13 living bats
GenBank accession numbers and percentages of genetic identification are presented, along with the species and origin of isolate. Number of isolates corresponds to the number of plates that grew a colony of the species. This relates directly to the number of bats a microbe was isolated from.

1.3.4 Hemolysis testing

Hemolysis testing was performed with two of the yeast isolated from the wings to determine virulence of the species present compared with *Pd* (Table 4). All three yeasts budded on blood agar plates. *Trichosporon* was the only species to demonstrate complete hemolysis (Beta hemolysis) on blood agar with and without glucose by week 6. *Candida* showed incomplete hemolysis (Alpha hemolysis) at week 2, and week 6. *Pd* was the only species to sporulate on the plates, but demonstrated only incomplete hemolysis (Alpha hemolysis) by week 6.

1.4 Discussion

Emerging infectious diseases have become an increasing concern for wildlife management (Daszak et al. 2000, Fisher et al. 2012), and among North American bats, WNS has caused massive population declines and has been identified as a severe threat to species persistence (Frick et al. 2010). It is therefore with alarm that I report the observation of another deadly disease affecting bats during hibernation. Signs of the disease comprised the rapid development of wing necroses including liquid-filled vesicles or deterioration of melanized skin, exposure of clear connective tissue, or loss of wing tissue, accompanied by blue fluorescence under ultraviolet light. Mortality was exceptionally high relative to typical levels observed during hibernation (Fritze & Puechmaille 2018), and began well prior to the typical seasonal timing of mortality from WNS. Further, during rehabilitation, disease effects in surviving bats were persistent for weeks after the end of hibernation, and mortality continued despite supportive care in euthermy that would normally be sufficient to enable all but bats with the most severe WNS infection to recover (S. Stronsick, pers. obs.). Thus, this disease, apparently

unknown prior to this study, appears even more aggressive than WNS, and adds to the already high level of concern for the conservation of North American hibernating bats.

	Week 1			
	No Glucose		Glucose	
Strain	Sporulation	Hemolysis	Sporulation	Hemolysis
Candida glaebosa	0	Gamma	0	Gamma
Trichosporon sp.	0	Gamma	0	Gamma
Pseudogymnoascus destructans	0	Gamma	2	Gamma
	Week 2			
	No Glucose		Glucose	
Strain	Sporulation	Hemolysis	Sporulation	Hemolysis
Candida glaebosa	0	Alpha / Beta	0	Alpha
Trichosporon sp.	0	Alpha / Beta	0	Alpha / Beta
Pseudogymnoascus destructans	2	Alpha	2	Alpha
	Week 6			
	No Glucose		Glucose	
Strain	Sporulation	Hemolysis	Sporulation	Hemolysis
Candida glaebosa	0	Alpha	0	Alpha
Trichosporon sp.	0	Beta	0	Beta
Pseudogymnoascus destructans	1	Alpha	3	Alpha

Table 4. Results of hemolysis testing Results of hemolysis testing of two yeasts isolated from bats in this study, compared with *Pd*. Gamma hemolysis is the equivalent of no hemolysis. Alpha hemolysis is incomplete hemolysis and is expressed as a darkened halo around the fungal colony. Beta hemolysis is complete hemolysis and is expressed as a clear ring around the fungal colony. Sporulation of the fungi was also examined, and only seen to occur in the *Pd* colonies.

1.4.1 Differences between observed disease and WNS

Even though the bats in this experiment were highly susceptible to WNS (Frank et al. 2014), and were experimentally exposed to *Pd* as part of a planned study, several lines of evidence indicate that WNS was not the primary cause of the observed disease impacts on bats in the study. First, the disease pathology of the observed bats differed from the pathology characteristic of WNS. During infection with WNS, connective tissue is digested and replaced with hyphae as *Pd* expands its colony (Meteyer et al. 2009). White hyphal growth becomes evident on the surface of the wing, and the wing loses its elasticity and tone in scattered locations, giving it the appearance of crumpled tissue paper (Cryan et al. 2010). In contrast, several bats in this study exhibited wing vesicles that progressively grew in size and resulted in deterioration of epidermal layers of wing skin (Figure 3). The digestion of epidermal layers and exposure of large areas of connective tissue to air was also common, but the wing itself did not lose its elasticity or shape until areas of exposed dermis desiccated and flaked off leaving holes in the wing (Figure 3E & 3F).

Second, when wings were trans-illuminated with UV light, orange-yellow fluorescence associated with WNS infection was not observed. In WNS infections, fungal hyphae fill epidermal cup-like erosions in the wing (Meteyer et al. 2009), and these erosions fluoresce orange-yellow in UV light (Figure 1F) (Turner et al. 2014). In contrast, blue fluorescence was seen in areas of edema in the wings of the bats in this study (Figure 1B & 1C). The epidermis of large sections of the wing was destroyed, exposing connective tissue and elastin underneath, which fluoresced bluish-white (Figure 3C & 3E,

black arrows). In addition, there was blue fluorescence in vesicles within the layers of skin of the wing (Figure 3B & 3C, arrowheads).

Third, the amount of infection with WNS that was seen was minimal during the short duration of the study. Although an examination of bat wings with UV light revealed some fluorescence in wavelengths characteristic of invasion by *Pd* (Turner et al. 2014), the total fluorescent area (both wings combined) of the wings never exceeded 0.1% in any bats throughout the experiment (Supplementary Table B2). This low level of infection at an early stage of the hibernation period (29 days for juveniles, 49 days for adults) is consistent with early hibernation progression of WNS reported in multiple studies (McGuire et al. 2016, Verant et al. 2014). McGuire et al. (2016) did not see any UV fluorescence, wing necrosis or fungal hyphae appear in the wings until after 60 days in hibernation, and there was a dramatic increase in all three after 90 days in hibernation (up to 40% of the plagiopatagium area fluoresced orange-yellow under UV). Similarly, in Verant et al. (2014), only two bats out of 39 inoculated with *Pd* displayed moderate to severe WNS infection after 98 days in hibernation; 30 displayed mild WNS infection, and seven displayed no infection at all – though they tested positive in qPCR for the presence of *Pd* genetic material. These studies describe an abrupt disruption of homeostasis occurring late in hibernation, related to worsening WNS-associated wing pathology. In contrast, in this study, severe impacts occurred much earlier – within weeks of the onset of hibernation.

Finally, mortality events occurred far earlier from the observed infection than typical mortality associated with WNS. Based on the timing of submissions for bat diagnostic testing associated with bat mortality, major WNS-associated mortality events

have not typically been reported seasonally until 120 days into hibernation (end of January in the northern USA), and do not peak until 180 days (in March) (Lorch et al. 2011). In contrast, in this study, the majority of juveniles (60%) were deceased by week 4 (after 29 days of hibernation) and the majority of adults (66.67%) deceased by week 7 (after 49 days of hibernation), suggesting that the observed disease is more aggressive, and has the ability to cause rapid mortality.

These factors strongly suggest WNS was not the cause. It is also unlikely that the observed signs could have been due to the experimental design, for at least three reasons. First, analysis of the data did not determine an effect of monitoring category on change in SMI or wing damage. Second, the disease signs observed in this study were not observed in a separate study by the same team of researchers (Gagnon et al., unpublished) that used different capture and experimental locations, but was conducted on the same bat species, in the same winter, and using nearly the same capture, transport, *Pd* exposure, and captive overwintering methods. Third, in this study, bat condition continued to worsen throughout the experimental period, and did not quickly alleviate among surviving bats, even after being maintained in euthermy, and provided supportive care by an experienced bat rehabilitator, unlike other bats cared for separately at the same center.

1.4.2 Host factors associated with disease severity

The body condition of healthy little brown myotis declines naturally during the hibernation period, while bats are in torpor. In previous experiments, the body condition of little brown myotis has been seen to decline an average of 30.7% in adult males and 32.8% in juvenile males during a hibernation season lasting 211 days (Jonasson and Willis 2011). Both the adult and juvenile males in this study saw an average decrease in

body condition of around 20% - 25% despite spending only 29 days in hibernation for juveniles, and 49 days for adults. The disease that was observed resulted in a much more rapid rate of body condition loss than what occurs in healthy little brown myotis in torpor (Jonasson and Willis 2011). Mortality also occurred at a faster rate among juveniles in this study than adults, suggesting the potential of this disease to reduce recruitment into the adult population.

1.4.3 Blue fluorescence

While I saw only minimal areas of orange-yellow fluorescence (Supplementary Table B2) that is associate with *Pd* fungal hyphae in cupping erosions (Turner et al. 2014), I did see blue fluorescence when wings were trans-illuminated with a UV lamp (368 nm) (Figures 1, 2, 3). Some of the blue fluorescence seen in the bats' wings appeared similar to vitiligo patches in human skin that fluoresce bright bluish-white when illuminated with a Wood's lamp (365 nm) (Klatte et al. 2014). Vitiligo is a disorder in which skin loses its melanocytes, resulting in depigmented patches (Klatte et al. 2014). The loss of epidermal melanin in these patches allows UV light to reach the connective tissue underneath the epidermis. In human skin, connective tissue in the dermis is composed of collagen, elastin, and other components including vasculature, nerve endings, hair follicles and sebaceous glands (Menon 2002). The extracellular fibrous protein elastin fluoresces light blue (420 nm – 510 nm) when illuminated with a Wood's lamp (Koenig and Schneckenburger 1993, Croce and Bottiroli 2014). The skin covering bat wings is composed of two thin layers of epidermis (only a few cells thick each) separated by a core of connective tissue with a central capillary network (Makanya and Mortola 2007). A bat's body epidermis alone is thicker than all of the layers that compose

the wing skin combined (Makanya and Mortola 2007). The core connective tissue of the wings is mostly made up of elastin and collagen fibers (Makanya and Mortola 2007). Similarly to humans, when the keratinized epidermal layers are removed from bat wings, the exposed elastin fluoresces bluish-white under UV light.

Blue fluorescence was additionally seen in another pathological sign of the infection - vesicles in the wings (Figure 3C, arrowhead). It was discovered through post-mortem examination that these vesicles were localized areas of yeast and fungal hyphae packed together, elevating the epidermis away from the connective tissue (Figure 6A). However, *Trichosporon sp*., like the yeast found in these vesicles, does not fluoresce when illuminated with UV by a Wood's lamp (Kiken et al. 2006). One possible explanation for the blue fluorescence generated in these vesicles is the association of bacteria that fluoresce in UV with the fungal elements inside the vesicles. Bacteria and fungi can exhibit a wide range of synergistic and antagonistic interactions (Hogan and Kolter 2002). The bacteria *Pseudomonas aeruginosa* has been documented to be pathogenic to *Candida albicans,* despite the fact that both appear as commensals in the skin microflora of healthy humans (Hogan and Kolter 2002). *C. albicans* exists in two forms – as a yeast and as filamentous cells. *Trichosporon* shares this characteristic with *C. albicans;* it exhibits phenotypic plasticity in its ability to grow as a budding yeast, or filamentous septate hyphae (Duarte-Oliveira et al. 2017). In the pathogenic relationship witnessed by Hogan and Kolter (2002), *P. aeruginosa* readily attached to *C. albicans* filaments and ultimately formed biofilms on the hyphae, extracting its nutrients, but almost never attached to the yeast form. *Pseudomonas fluorescens* displayed a similar capacity to *P. aeruginosa*, although the interaction was synergistic rather than

antagonistic. *Pseudomonas fluorescens* have been seen to attach to living hyphae of arbuscular mycorrhizal fungi *Glomus sp*. (Toljander et al. 2006). *Pseudomonas fluorescens* has also been proposed as a probiotic treatment to fight WNS in bats because of the microbe's ability to produce a suite of antifungal compounds like mycolysing enzymes (Hoyt et al. 2015). *Pseudomonas fluorescens* is one of a few *Pseudomonas* species which produce fluorescent siderophores pyocyanin and pyoverdine (Ward et al. 1967). Pyoverdine, or fluorescein, is a virulence factor for the bacteria and produces a blue to yellow-green fluorescence under UV light illumination (Wasserman et al. 1965, Meyer and Abdallah 1978). *Pseudomonas fluorescens* emits a range of fluorescence from yellow-green to dull blue when grown on different nutrient agars and at different pH levels (Wasserman et al. 1965, Meyer and Abdallah 1978). Several *Pseudomonas* species were found on the wings of the bats in this study including *P. fluorescens* (Table 3). Given its capacity for attachment to and colonization of fungal hyphae, it is possible that *P. fluorescens* attached to the *Trichosporon* hyphae found in the wing vesicles (Figure 3C, arrowhead), giving them a blue-green glow when illuminated with UV light. However, further investigation is needed to clarify the source of this fluorescence.

1.4.4 Isolated fungi and bacteria

Trichosporon species are basidiomycetous yeast-like anamorphic organisms that are widely distributed in nature and are predominately found in substrates like soil and decomposing wood (Chagas-Neto et al. 2008). The fungus is characterized by its ability to form true hyphae and pseudohyphae, blastoconidia and arthroconidia (Pfaller et al. 2009). *Trichosporon* are commonly isolated from cave environments (Sugita et al. 2005, Lorch et al. 2013, Zhang et al. 2014), and have been documented to be part of the

external microbiota of healthy bats (Voyron et al. 2011, Johnson et al. 2013, Vanderwolf et al. 2013, Holz et al. 2018). In fact, the *Trichosporon* species that was isolated from the ears, wings and muzzle of one of the study bats was first identified by Lorch et al. (2013) in a soil sample taken from a New Hampshire hibernaculum. The ability of *Trichosporon* species to act as opportunistic pathogens has been more widely recognized in recent years as a result of the reevaluation of their taxonomy (Guého et al. 1992, Mariné et al. 2015), and increased incidence of *Trichosporon* mycoses in immunocompromised patients (Chagas-Neto et al. 2008, Pfaller et al. 2009) and a few immunocompetent patients (Pulvirenti et al. 2006, Mariné et al. 2015). Since they are part of the natural microbiota of humans, *Trichosporon* species may have been considered contaminants in clinical investigations, when they could have actually been the etiological agent in an estimated 10% - 40% of superficial infections, depending on the geographic area and population (Mariné et al. 2015). *Trichosporon* infections of animals have increased as well, including disseminated trichosporosis in cats, canine meningitis, and tortoise cutaneous infections (Ma et al. 2019).

Other fungi that were isolated from the wings included a *Penicillium* sp., *Mucor saturninus*, *Candida glaebosa*, and *Rhodotorula mucilaginosa* (Table 1, Table 3). *Penicillium* are one of the most abundant fungi genera isolated from cave environments (Adetutu et al. 2011, Lorch et al. 2013, Zhang et al. 2014), and from bats (Voyron et al. 2011, Johnson et al. 2013, Vanderwolf et al. 2013). They are saprotrophic fungi, known for their cold tolerance, that decompose organic matter and return nutrients back into cave ecosystems (Adetutu et al. 2011). Their presence on the bats likely results from the state of decomposition the bats were in when sent to the SCWDS veterinarians at the

University of Georgia. As saprotrophic fungi, the presence of *Penicillium* is attributed to post-mortem overgrowth of the bat carcasses, and not thought of as a pathogen associated with the disease described. *Mucor saturninus* was first isolated from decaying mushrooms and soil (Walther et al. 2013). No case reports have been published demonstrating *M. saturninus* to be infectious, and its presence on the deceased bats is attributed to its role as saprotrophic environmental fungi (Walther et al. 2013). *Candida glaebosa* has been isolated from frozen and fermented foods (Komagata and Nakase 1965, Ryun et al. 2012, Kivanç and Yapici 2015). The species has not been identified as a clinically important pathogen, and it likely constitutes an environmental contaminant, unrelated to the observed disease (Criseo et al. 2015, Shokohi et al. 2018). Lastly, *Rhodotorula mucilaginosa* was isolated from the wings of three bats in this study (Table 3). This ubiquitous saprophytic yeast has been recovered from numerous environmental sources (Wirth and Goldani 2012). *Rhodotorula mucilaginosa* has been identified as an emerging pathogen of humans and animals in recent years (Beemer et al. 1970, Perniola et al. 2006, Wirth and Goldani 2012). However, *R. mucilaginosa* does not have the ability to form hyphae (Wirth and Goldani 2012). The presence of hyphae within the wing epidermis and vesicles in the wing, lead us to believe that *Trichosporon*, rather than *R. mucilaginosa* was the fungal pathogen associated with the observed wing damage.

Although numerous bacterial species with varying degrees of pathogenicity were found in this study, only a few were found internally, and only one was found in all of the organs examined as well as on the surface of the wing. The species that were found internally include *Lactococcus raffinolactis* (liver), *Hafnia alvei* (liver), *Carnobacterium maltaromaticum* (heart, kidney), *Pseudomonas brenneri* (heart, lung), and *Serratia*

liquefaciens (heart, kidney, liver, lung) (Table 1; Table 2). Of the species found internally, *H. alvei, C. maltaromaticum, P. brenneri,* and a *Serratia* species were also found on the wings (Table 2, Table 3). Because of their presence both internally and externally, these four species are more closely examined in this analysis. This does not eliminate the possibility of involvement in the infection by other identified bacteria species. It is possible that individual bats experienced different secondary bacterial infections leading to a similar outcome. The systemic presence of these species simply makes them more likely to be part of the mortality that resulted in the study, though not all of these species are equally likely to lead to death.

Hafnia alvei, while considered a commensal of the human gastrointestinal flora, has been suggested to play a role as an opportunistic pathogen (Podschun et al. 2001). But low expression of virulence factors suggest that *H. alvei* has minimal pathogenicity compared to other members of the order Enterobacterales (Podschun et al. 2001). However, septicemia in hens has been attributed to *H. alvei* (Real et al. 1997). Given the low pathogenicity, and the isolation of *H. alvei* from only the liver, it is unlikely that this species led to the death of most of the bats in this study. Also, *H. alvei* was not recovered from the wing swabs taken from living bats; it was only seen on the bat carcasses, leading us to believe that its presence was post-mortem overgrowth.

Although Gram-positive *Carnobacterium maltaromaticum* has been associated with disease in fish, it is not seen as a pathogen of humans or other mammals (Loch et al. 2008, Schaffer et al. 2012). It is more commonly seen in vacuum-packed or frozen food, or isolated from the environment (Leisner et al. 2007), and occasionally acts as an inhibitor of pathogenic bacteria (Ringa 2008). *Carnobacterium* have been isolated

internally from the gastrointestinal tract (Phillips et al. 2012, Banskar et al. 2016, Dietrich et al 2017), and externally from the forearm and muzzle of healthy little brown myotis (Avena et al. 2016), and from the air in cave environments (Mulec et al. 2017). Similarly to *H. alvei, C. maltaromaticum* was not isolated from the wing swabs of living bats, only from the bat carcasses. For these reasons, *C. maltaromaticum* is presumed to be a contaminant rather than a pathogen and, as proposed in the SCWDS reports, is likely the result of post-mortem overgrowth.

Pseudomonas species were abundantly isolated from the wings of the little brown myotis in this study, however, only *Pseudomonas brenneri* was found internally (Table 2, Table 3). This bacterial genus is one of the most commonly isolated from bats both externally (Zenowiak et al. 1993, Voigt et al. 2005, Hoyt et al. 2015, Avena et al. 2016, Hamm et al. 2017, Gaona et al. 2019, Grisnik et al. 2020) and internally (Dietrich et al. 2017, Cláudio et al. 2018, Vengust et al. 2018, Selvin et al. 2019), and from the environment as well, although with slightly less frequency (Barton et al. 2007). *Pseudomonas brenneri* was originally isolated from mineral water (Baïda et al. 2001), and has since been isolated from coal mine wastewater; it is proposed to be a biochemical remediator, like a few other species of *Pseudomonas* (Banerjee et al. 2019). The three *Pseudomonas* species identified in this study (*P. brenneri*, *P. fluorescens*, and *P. gessardii*) have all been classified to the *Pseudomonas fluorescens* group based on 16S rDNA sequences (Van den Beld et al. 2016); however, a recent multilocus sequence analysis (MLSA) has reclassified this group as the *P. fluorescens* complex and split it into multiple subgroups. The reclassification separated the *P. fluorescens* group from the *P. gessardii* group, which also contains *P. brenneri* (Garrido-Sanz et al. 2016). Members

of the *P. fluorescens* complex are Gram-negative, rod shaped bacteria that share characteristics like production of pyoverdine, fluorescent pigment molecules (Baïda et al. 2001). The species in this complex have all displayed mycelial inhibition of molds and rot of commercially important fruits and vegetables in storage (Luo et al. 2019); several have also been described as plant growth-promoting rhizobacteria (PGPR) (Garrido-Sanz et al. 2016). They are not described as pathogenic to mammals (Scales et al. 2014), and none of the species exhibit complete hemolysis (Van den Beld et al. 2016), but they can be antagonists of fungi, as seen through their ability to inhibit mold and rot (Luo et al. 2019). Although likely responsible for the fluorescence seen in the wing vesicles through their attachment to fungal hyphae, the *Pseudomonas* species isolated are unlikely to have played a role in the infection of bats in this study. There were, however, two unidentified *Pseudomonas* species isolated from the wings of bats in this study. If these species belong to another *Pseudomonas* group other than the *P. fluorescens* group, they could have greater pathogenicity in mammals. Ultimately, only one species appeared both internally and externally on the bats and that was *P. brenneri*, an unlikely pathogen and a probable environmental contaminant.

Serratia are ubiquitous in the environment and have been isolated from water, soil, animals, insects, and plants (Mahlen 2011). *Serratia* species, especially *S. marcescens*, but also *S. liquefaciens*, are an important cause of animal diseases (Mahlen 2011). *Serratia* species have been documented to cause nosocomial infections in humans related to infected equipment, medical devices and procedures in hospitals (Mahlen 2011, Ikumapayi et al. 2016). *Serratia liquefaciens*, the second most common species isolated from human clinical samples after *S. marcescens*, may be underestimated in its clinical

significance due to multiple changes in its classification over time (Mahlen 2011). Transfusion-related sepsis due to *S. liquefaciens* has been documented in the United States and has led to a high mortality rate (Roth et al. 2000). Although colony-forming units (CFUs) in the blood of the infected bats were not measured, *S. liquefaciens* was isolated from the heart, kidney, lung and liver of an individual bat, indicating that the species was wide-spread throughout various organ systems of the body. And its presence in the heart and blood vessels strongly indicates its presence in the blood stream of infected bats.

1.4.5 Host characteristics influencing disease onset and progression

Because the fungal and bacterial species identified as possible etiological agents occurred on bats in all four experimental groups – each in a separate, non-adjacent cage in the experimental site – I believe that they were likely already on the bats prior to the start of the experiment (perhaps transmitted among bats during interactions at the single maternity colony where all bats in this study were captured), and immunosuppression by the bats while in hibernation (Field et al. 2018) may have partially allowed for an opportunistic infection. Metabolically costly immune responses are downregulated during hibernation by bats in order to conserve energy (Meteyer et al. 2012). When in torpor, circulating leukocytes are decreased by about 90% in all hibernating mammals studied so far, and the decrease may significantly reduce the acute inflammatory response of the animal, rendering it unable to clear itself of pathogenic microbes (Bouma et al. 2010). Additionally, it was recently discovered that *Trichosporon* species can produce Glucuronoxylomannan (GXM), a well-known virulence factor of *Cryptococcu*s yeasts (Fonseca et al. 2009, Mariné et al. 2015). *Cryptococcus* yeasts are another invasive

dermatophyte commonly associated with human infection (Fonseca et al. 2009). GXM is a polysaccharide produced by yeasts that protects its cells from phagocytosis (Fonseca et al. 2009), and helps the pathogen evade detection by the immune system of the infected host, which would already have been downregulated by the bats in this study (Mariné et al. 2015). The ability of *Trichosporon* sp. to produce GXM aids in its capacity to evade what remains of the host's immune responses (Mariné et al. 2015).

Many of the microbes described here are frequently found to be part of the bat microbiota, or found environmentally in cave substrates, and under typical circumstances may not pose a severe threat to bats. After infection with one disease, however, a host may become more susceptible to other pathogens. For instance, during advanced infection of sea star hosts with Sea Star Wasting Disease, the host epidermal microbiome exhibited reduced microbial diversity, decreases in beneficial microbes, and increases in pathogenic or opportunistically pathogenic microbes (Lloyd & Pespeni 2018). Similar changes in host microbiomes were driven by chytrid fungal infections in frogs (Jani & Briggs 2014). Coming from a county where WNS has been detected since 2009, the bats in this study have likely experienced and survived infection with *Pd*, perhaps repeatedly. The decrease in commensal bacterial species on the surface of the wing could have allowed for colonization by an opportunistic pathogen developing into the observed infection. It is also possible that bats collected for this study from the maternity colony were already dealing with other unidentified stressors, rendering them immunocompromised. While the precise reason for the onset of the observed infection remains unclear, polymicrobial infections of hibernating little brown myotis could account for both the rapid deterioration of the wings and the high degree of mortality.

1.4.6 Hypothesized disease agents

Although I am unable to attribute the observed disease to specific etiological agents without fulfilling Koch's postulates (Koch 1884), I suspect that a polymicrobial infection led to the pathology described in this paper. The cutaneous damage seen in the wings, though different from *Pd* invasion, is likely the result of the aggregated yeast, and fungal hyphae found in the wings. *Trichosporon sp.*, occurring across the wing, in wing vesicles, and throughout the ear and muzzle skin (Figure 6), is thought to be the fungal pathogen responsible for the observed damage. Although *Trichosporon* was not found in wing swabs taken from the bats, this may be due to cold storage of the swabs in a freezer that went through cycles of freezing and thawing, which can cause some fungal spores to lose viability (Thammavongs et al. 2000). Multiple *Trichosporon* species have pathogenic traits that allow for them to invade skin and other tissues; those traits include the ability to form biofilms (Di Bonaventura et al. 2006), production of enzymes like phospholipases and proteases, and the production of hyphae and pseudohyphae (Mariné et al. 2015). Like other fungal pathogens, *Trichosporon* species produce phospholipases, allowing them to break down cell walls, and proteases which play a major role in overcoming host immunological barriers (Mariné et al. 2015). And as previously mentioned, the ability of *Trichosporon* sp. to produce GXM allows it to avoid phagocytosis by the host's immune system (Mariné et al. 2015). Hemolysis testing was also conducted to examine additional factors contributing to the interaction between *Trichosporon* and its bat hosts (Table 4). *Trichosporon* displayed incomplete hemolysis in the second week of the experiment, but complete hemolysis by the 6th week, showing its capacity to lyse red blood cells quickly. This ability could explain the hemorrhage

observed over areas of edema in the wings as reported by the veterinarians that examined the bats post-mortem at SCWDS.

While there were multiple bacterial species with pathogenic potential isolated from the wings of the bats (Table 3), only a *Serratia* species was isolated internally as well. *Serratia liquefaciens*, specifically, was isolated from every organ examined – heart, kidney, liver, lung (Table 2). There were also small rod-shaped bacterial colonies, consistent with *Serratia* morphology, seen throughout the organ systems and within the dermis and blood vessels, as reported by veterinarians at SCWDS. The widespread presence of this bacterium suggests its potential pathological importance in the observed infection. And the positive association found between *Serratia* sp. and fungal infections in other wildlife species (Allender et al. 2018) may suggest a propensity of this bacterium to take advantage of skin lesions created by fungal pathogens. Previous studies have also documented simultaneous bacterial-fungal infections that have led to enhanced killing, where the infected host died more rapidly when infected with both pathogens, than with either species individually (Peleg et al. 2010). I therefore hypothesize that *Trichosporon* created the initial invasion of skin tissue, allowing for secondary bacterial infection by *Serratia* and subsequent sepsis in the host.

1.5 Conclusion

Hibernating bats in North America have undergone severe declines in recent years (Thogmartin et al. 2012, Ingersoll et al. 2013). These declines have often been assumed to be solely due to WNS (e.g., USFWS 2012). It is clear that WNS has been a key factor in these declines, but WNS alone does not explain all of the population changes in bats (Ingersoll et al. 2013, Ingersoll et al. 2016). Bats face a diversity of important non-disease

related threats (Ingersoll et al. 2013). Meanwhile, new threats to bats continue to be identified, including the recent discovery of a dermatophyte – *Trichophyton redellii* – that causes clinical infections in bats that present similarly to WNS (Lorch et al. 2015). In this study, I provided the first description of the pathology of a previously undetected disease affecting bats, one that is highly aggressive and likely polymicrobial in nature, that led to extensive wing damage and mortality at an even more rapid rate than WNS. I identified potential causal agents of the disease, but future research should examine the etiological agents proposed in this study to clarify their role in disease progression and mortality. This research further underlines the precarious status of many North American bat populations. Even as WNS and other known threats cause massive declines, new threats lurk, and synergistic effects among these threats could compound bat population losses (Hilker et al. 2009, Luarance & Useche 2009). These losses may even lead to the extirpation of small or isolated bat colonies. It is therefore imperative that managers and biologists act quickly to promote the recovery of extant bat populations, while also remaining vigilant to known and emerging threats to North American bats.

REFERENCES CITED

Adetutu E.M., Thorpe K., Bourne S., Cao X., Shahsavari E., Kirby G. & Ball A.S. (2011). Phylogenetic diversity of fungal communities in areas accessible and not accessible to tourists in Naracoorte Caves. Mycologia 103(5): 959-968.

Aktas E. & Yigit N. (2015). Hemolytic activity of dermatophyte species isolated from clinical specimens. Journal de Mycologie Médicale 25: e25-e30.

Allender M.C., Baker S., Britton M. & Kent A.D. (2018). Snake fungal disease alters skin bacterial and fungal diversity in an endangered rattlesnake. Scientific Reports 8: 12147.

Avena C.V., Parfrey L.W., Leff J.W., Archer H.M., Frick W.F., Langwig K.E., Kilpatrick A.M., Powers K.E., Foster J.T. & KcKenzie V.J. (2016). Deconstructing the bat skin microbiome: influences of the host and the environment. Frontiers in Microbiology 7: 1753.

Baïda N., Yazourh A., Singer E. & Izard D. (2001). *Pseudomonas* brenneri sp. nov., a new species isolated from natural mineral waters. Research in Microbiology 152(5): 493-502.

Banerjee S., Kamila B., Barman S., Joshi S.R., Mandal T. & Halder G. (2019). Interlining Cr(VI) remediation mechanism by a novel bacterium *Pseudomonas brenneri* isolated from coalmine wastewater. Journal of Environmental Management 233: 271-282.

Banskar S., Bhute S.S., Suryavanshi M.V., Punekar S. & Shouche Y.S. (2016). Microbiome analysis reveals the abundance of bacterial pathogens in *Rousettus leschenaultii* guano. Scientific Reports 6: 36948.

Barton H.A., Taylor N.M., Kreate M.P., Springer A.C., Oehrle S.A. & Bertog J.L. (2007). The impact of host rock geochemistry on bacterial community structure in oligotrophic cave environments. International Journal of Speleology 36(2): 93-104.

Beemer A.M., Schneerson-Porat S. & Kuttin E.S. (1970). *Rhodotorula mucilaginosa* dermatitis on feathered parts of chickens: an epizootic on a poultry farm. Avian Diseases 14(2): 234-239.

Blehert D.S., Hicks A.C., Behr M., Meteyer C.U., Berlowski-Zier B.M., Buckles E.L., Coleman J.T.H, Darling S.R., Gargas A., Niver R., Okoniewski J.C., Rudd R.J. & Stone W.B. (2009). Bat white-nose syndrome: an emerging fungal pathogen? Science 323(5911): 227.

Bohonak A.J. & Van der Linde K. (2004). RMA: software for reduced major axis regression, Java version./<www.kimvdlinde.com/professional/rma.html/>; accessed 11 July 2020.

Bouma H.R., Carey H.V. & Kroese F.G.M. (2010). Hibernation: the immune system at rest? Journal of Leukocyte Biology 88: 619-624.

Calisher C.H., Childs J.E., Field H.E., Holmes K.V. & Schountz T. (2006). Bats: important reservoir hosts of emerging viruses. Clinical Microbiology Reviews 19(3): 531-545.

Chagas-Neto T.C., Chaves G.M. & Colombo A.L. (2008). Update on the genus *Trichosporon*. Mycopathologia 166: 121-132.

Chappell W.A. & Titman R.D. (1983). Estimating reserve lipids in greater scaup (*Authua marila*) and lesser scaup (*A. affinis*). Canadian Journal of Zoology 61(1): 35-38.

Chothe, S.K., G. Bhushan, R. H. Nissly, Y-T. Yeh, J. Brown, G. Turner, J. Fisher, B. J. Sewall, D. M. Reeder, M. Terrones, B. M. JayaRao and S. V. Kuchipudi 2017. Avian and human influenza virus compatible sialic acid receptors in little brown bats. Scientific Reports 7: 660.

Cláudio V.C., Gonzalez I., Barbosa G., Rocha V., Moratelli R. & Rassy F. (2018). Bacteria richness and antibiotic-resistance in bats from a protected area in the atlantic forest of southeastern Brazil. PLoS ONE 13(9): e0203411.

Criseo G., Scordino F. & Romeo O. (2015). Current methods for identifying clinically important cryptic *Candida* species. Journal of Microbiological Methods 111: 50-56.

Croce A.C. & Bottiroli G. (2014). Autofluorescence spectroscopy and imaging: a tool for biomedical research and diagnosis. European Journal of Histochemistry 58(2461): 320-337.

Cryan P.M., Meteyer C.U., Boyles J.G. & Blehert D.S. (2010). Wing pathology of white-nose syndrome in bats suggests life-threatening disruption of physiology. BMC Biology 8: 135.

Cryan P.M., Meteyer C.U., Blehert D.S., Lorch J.M., Reeder D.M., Turner G.G., Webb J., Behr M., Verant M., Russell R.E. & Castle K.T. (2013). Electrolyte Depletion in White-nose Syndrome Bats. Journal of Wildlife Diseases 49(2): 398-402.

Daszak P., Cunningham A.A. & Hyatt A.D. (2000). Wildlife ecology - Emerging infectious diseases of wildlife - Threats to biodiversity and human health. Science 287: 443-449.

Di Bonaventura G., Pompilio A., Picciani C., Iezzi M., D'Antonio D. & Piccolomini R. (2006). Biofilm formation by the emerging fungal pathogen *Trichosporon asahii*: development, architecture, and antifungal resistance. Antimicrobial Agents and Chemotherapy 50(10): 3269-3276.

Dietrich M., Kearney T., Seamark E.C.J. & Markotter W. (2017). The excreted microbiota of bats: evidence of niche specialisation based on multiple body habitats. FEMS Microbiology Letters 364: fnw284.

Duarte-Oliveira C., Rodrigues F., Gonçalves S.M., Goldman G.H., Carvalho A., Cunha C. (2017). The cell biology of the *Trichosporon*-Host interaction. Frontiers in Cellular and Infection Microbiology 7: 118.

Fey S.B., Siepielski A.M., Nusslé S., Cervantes-Yoshida K., Hwan J.L., Huber E.R., Fey M.J., Catenazzi A. & Carlson S.M. (2015). Recent shifts in the occurrence, cause and magnitude of animal mass mortality events. PNAS 112(4): 1083-1088.

Field K.A., Johnson J.S., Lilley T.M., Reeder S.M., Rogers E.J., Behr M.J. & Reeder D.M. (2015). The white-nose syndrome transcriptome: activation of antifungal host responses in wing tissue of hibernating little brown myotis. PLoS Pathog 11(10): e1005168.

Field, K.A., Sewall B.J., Prokkola J.M., Turner G.G., Gagnon M.F., Lilley T.M., White J.P., Johnson J.S., Hauer C.L. & Reeder D.M. (2018). Effect of torpor on host transcriptomic responses to a fungal pathogen in hibernating bats. Molecular Ecology 27: 3727-3743.

Fisher M.C., Henk D.A., Briggs C.J., Brownstein J.S., Madoff L.C., McCraw S.L. & Gurr S.J. (2012). Emerging fungal threats to animal, plant and ecosystem health. Nature 484: 186-194.

Fonseca F.L., Frases S., Casadevall A., Fischman-Gompertz O., Nimricter L. & Rodrigues M.L. (2009). Structural and functional properties of the *Trichosporon asahii* glucuronoxylomannan. Fungal Genetics and Biology 46(0): 496-505.

Frank C.L., Michalski A., McDonough A.A., Rahimian M., Rudd R.J. & Herzog C. (2014). The Resistance of a North American Bat Species (*Eptesicus fuscus*) to White-Nose Syndrome (WNS). PLoS ONE 9.

Frick W.F., Pollock J.F., Hicks A.C., Langwig K.E., Reynolds D.S., Turner G.G., Butchkoski C.M. & Kunz T.H. (2010). An emerging disease causes regional population collapse of a common North American bat species. Science 329: 679-682.

Frick W.F., Puechmaille S.J., Hoyt J.R., Nickel B.A., Langwig K.E., Foster J.T., Barlow Ǩ.E., Bartonicka T., Feller D., Haarsma A.J., Heřzog C., Horácek I., Van der Kooij J., Mulkens B., Petrov B., Reynolds R., Rodrigues L., Stihler C.W., Turner G.G. & Kilpatrick A.M. (2015). Disease alters macroecological patterns of North American bats. Global Ecology and Biogeography 24: 741-749.

Fritze M. & Puechmaille S.J. (2018). Identifying unusual mortality events in bats: a baseline for bat hibernation monitoring and white-nose syndrome research. Mammal Review 48: 224-228.

Gaona O., Cerqueda-García D., Falcón L.I., Vázquez-Domínguez G., Valdespino-Castillo P.M. & Neri-Barrios C.X. (2019). Microbiota composition of the dorsal patch of reproductive male *Leptonycteris yerbabuenae*. PLoS ONE 14(12): e0226239.

Garrido-Sanz D., Meier-Kolthoff J.P., Göker M., Martin M., Rivilla R. & Redondo-Nieto M. (2016). Genomic and genetic diversity within the *Pseudomonas fluorescens* complex. PLoS ONE 11(2): e0150183.

Ghanem S.J. & Voigt C.C. (2012). Increasing Awareness of Ecosystem Services Provided by Bats. Advances in the Study of Behavior 44: 279-302.

Grieneisen L.E., Brownlee-Bouboulis S.A., Johnson J.S. & Reeder D.M. (2015). Sex and hibernaculum temperature predict survivorship in white-nose syndrome affected little brown myotis (*Myotis lucifugus*). Royal Society Open Science 2: 140470.

Grisnik M., Bowers O., Moore A.J., Jones B.F., Campbell J.R. & Walker D.M. (2020). The cutaneous microbiota of bats has *in vitro* antifungal activity against the white nose pathogen. FEMS Microbiology Ecology 96(2): fiz193.

Guého E., de Hoog G.S. & Smith M.T. (1992). Neotypification of the genus *Trichosporon.* Antonie van Leeuwenhoek International Journal of General and Molecular Microbiology 61: 285-288.

Hamm P.S., Caimi N.A., Northup D.E., Valdez E.W., Buecher D.C., Dunlap C.A., Labeda D.P., Leuschow S. & Porras-Alfaro A. (2017). Western bats as a reservoir of novel *Streptomyces* species with antifungal activity. Applied and Environmental Microbiology 83(5): e03057-16.

Hilker F.M., Langlais M. & Malchow H. (2009). The Allee Effect and infectious diseases: extinction, multistability, and the (dis-)appearance of oscillations. The American Naturalist 173(1): 72-88.

Hogan D.A. & Kolter R. (2002). *Pseudomonas-Candida* interactions: an ecological role for virulence factors. Science 296: 2229-2232.

Holz P.H., Lumsden L.F., Marenda M.S., Browning G.F. & Hufschmid J. (2018). Two subspecies of bent-winged bats (*Miniopterus orianae bassanii* and *oceanensis*) in southern Australia have diverse fungal skin flora but not *Pseudogymnoascus destructans*. PLoS ONE 13(10): e0204282.

Hoyt J.R., Cheng T.L., Langwig K.E., Hee M.M., Frick W.F. & Kilpatrick A.M. (2015). Bacteria isolated from bats inhibit the growth of *Pseudogymnoascus destructans*, the causative agent of white-nose syndrome. PLoS ONE 10(4): e0121329.

Ingersoll T.E., Sewall B.J. & Amelon S.K. (2013). Improved analysis of long-term monitoring data demonstrates marked regional declines of bat populations in the eastern United States. PLoS ONE 8: e65907.

Ingersoll T.E., Sewall B.J. & Amelon S.K. (2016). Effects of white-nose syndrome on regional population patterns of 3 hibernating bat species. Conservation Biology 30: 1048-1059.

Ikumapayi U.N., Kanteh A., Manneh J., Lamin M. & Mackenzie G.A. (2016). An outbreak of *Serratia liquefaciens* at a rural health care in The Gambia. The Journal of Infection in Developing Countries 10(8): 791-798.

Jani A.J. & Briggs C.J. (2014). The pathogen *Batrachochytrium dendrobatidis* disturbs the frog skin microbiome during a natural epidemic and experimental infection. PNAS 111(47): E5049-E5058.

Johnson L.J.A., Miller A.N., McCleery R.A., McClanahan R., Kath J.A., Lueschow S. & Porras-Alfaro A. (2013). Psychrophilic and psychrotolerant fungi on bats and the presence of *Geomyces* spp. on bat wings prior to the arrival of white nose syndrome. Applied and Environmental Microbology 79(18): 5465-5471.

Jonasson K.A. & Willis C.K.R. (2011). Changes in body condition of hibernating bats support the Thrifty Female Hypothesis and predict consequences for populations with white-nose syndrome. PLoS ONE 6(6): e21061.

Kannan K,, Yun S.H., Rudd R.J. & Behr M. (2010) High concentrations of persistent organic pollutants including PCBs, DDT, PBDEs and PFOS in little brown bats with white-nose syndrome in New York, USA. Chemosphere 80: 613–618.

Kiken D.A., Sekaran A., Antaya R.J., Davis A., Imaeda S., Silverberg N.B. (2006). White piedra in children. Journal of the American Academy of Dermatology 55(6): 956-961.

Kivanç M. & Yapici E. (2015). Kefir as a probiotic dairy beverage: determination lactic acid bacteria and yeast. International Journal of Food Engineering 1(1): 55-60.

Klatte J.L., Van der Beek N. & Kemperman P.M.J.H. (2015). 100 years of Wood's lamp revised. Journal of the European Academy of Dermatology and Venereology 29: 842-847.

Knapp R.A., Fellers G.M., Kleeman P.M., Miller D.A.W., Vredenburg V.T., Rosenblum E.B. & Briggs C.J. (2016). Large-scale recovery of an endangered amphibian despite ongoing exposure to multiple stressors. PNAS 113(42): 11889-11894.

Koch, R. (1884). Die aetiologie der tuberkulose. Mitt. Kaiser. Gesundh. 2: 1–88.

Koenig K. & Schneckenburger H. (1994). Laser-induced autofluorescence for medical diagnosis. Journal of Fluorescence 4(1): 17-40.

Komagata K. & Nakase T. (1965). New species of the genus *Candida* isolated from frozen foods. Journal of General and Applied Microbiology 11(3): 255-267.

Kunz T.H. & Fenton M.B. (2003). Bat Ecology. Illinois: University of Chicago Press. 779p.

Kunz T.H., de Torrez E.B., Bauer D., Lobova T. & Fleming T.H. (2011). Ecosystem services provided by bats. Annals of the New York Academy of Sciences 1223: 1-38.

Langwig K.E., Frick W.F., Reynolds R., Parise K.L., Drees K.P., Hoyt J.R., Cheng T.L., Kunz T.H., Foster J.T. & Kilpatrick A.M. (2015). Host and pathogen ecology drive the seasonal dynamics of a fungal disease, white-nose syndrome. Proceedings of the Royal Society B 282: 20142335.

Laurance W.F. & Useche D.C. (2009) Environmental synergisms and extinctions of tropical species. Conservation Biology 23: 1427–1437.

Leisner J.J., Laursen B.G., Prévost H., Drider D. & Dalgaard P. (2007). Carnobacterium: positive and negative effects in the environment and in foods. FEMS Microbiology Reviews 31: 592-613.

Lilley T.M., Johnson J.S., Ruokolainen L., Rogers E.J., Wilson C.A., Schell S.M., Field K.A. & Reeder D.M. (2016). White-nose syndrome survivors do not exhibit frequent arousals associated with *Pseudogymnoascus destructans* infection. Frontiers in Zoology 13:12.

Lloyd M.M. & Pespeni M.H. (2018). Microbiome shifts with onset and progression of Sea Star Wasting Disease revealed through time course sampling. Scientific Reports 8(1): 16476.

Loch T.P., Xu W., Fitzgerald S.M. & Faisal M. (2008). Isolation of a *Carnobacterium maltaromaticum*-like bacterium from systemically infected lake whitefish (*Coregonus clupeaformis*). FEMS Microbiology Letters 288: 76-84.

Lorch J.M., Meteyer C.U., Behr M.J., Boyles J.G., Cryan P.M., Hicks A.C., Ballmann A.E., Coleman J.T.H., Redell D.N., Reeder D.M. & Blehert D.S. (2011). Experimental infection of bats with *Geomyces destructans* causes white-nose syndrome. Nature 480: 376-378.

Lorch J.M., Lindner D.L., Gargas A., Muller L.K., Minnis A.M. & Blehert D.S. (2013). A culture-based survey of fungi in soil from bat hibernacula in the eastern United States and its implications for detection of *Geomyces destructans*, the causal agent of bat white-nose syndrome. Mycologia 105(2): 237-252.

Lorch J.M., Minnis A.M., Meteyer C.U., Redell J.A., White J.P., Kaarakka H.M., Muller L.K., Lindner D.L., Verant M.L., Shearn-Bochsler V. & Blehert D.S. (2015). The fungus Trichophyton redellii sp. nov. causes skin infections that resemble white-nose syndrome of hibernating bats. Journal of Wildlife Diseases 51(1): 36-47.

Luo M., Purdy H. & Avis T.J. (2019). Compost bacteria provide antifungal activity against grey mold and *Alternaria* rot on bell pepper fruit. Botany 97: 221-230.

Ma X., Jiang Y., Wang C., Gu Y., Cao S., Huang X., Wen Y., Zhao Q., Wu R., Wen X., Yan Q., Han X., Zuo Z., Deng J., Ren Z., Yu S., Shen L., Zhong Z., Peng G., Liu H. & Zhou Z. (2019). Identification, genotyping, and pathogenicity of *Trichosporon* spp. isolated from giant pandas (*Ailuropoda melanoleuca*). BMC Microbiology 19: 113.

Mahlen S.D. (2011). *Serratia* infections: from military experiments to current practice. Clinical Microbiology Reviews 24(4): 755-791.

Makanya A.N. & Mortola J.P. (2007). The structural design of the bat wing web and its possible role in gas exchange. Journal of Anatomy 211: 687-697.

Mariné M., Brown N.A., Riaño-Pachón D.M. & Goldman G.H. (2015). On and under the skin: emerging basidiomycetous yeast infections caused by *Trichosporon* species. PLoS Pathogens 11(7): e1004982.

Martel A., Blooi M., Adriaensen C., Van Rooij P., Beukema W., Fisher M.C., Farrer R.A., Schmidt B.R., Tobler U., Goka K., Lips K.R., Muletz C., Zamudio K., Bosch J., Lötters S., Wombwell E., Garner T.W.J., Cunningham A.A., Spitzen-van der Sluijs A., Salvidio S., Ducatelle R., Nishikawa K., Nguyen T.T., Kolby J.E., Bocxlaer I.V., Bossuyt F. & Pasmans F. (2014). Recent introduction of a chytrid fungus endangers Western Palearctic salamanders. Science 346(6209): 630-631.

McGuire L.P., Turner J.M., Warnecke L., McGregor G., Bollinger T.K., Misra V., Foster J.T., Frick W.F., Kilpatrick A.M. & Willis C.K.R. (2016). White-nose syndrome disease severity and a comparison of diagnostic methods. EcoHealth 13: 60-71.

Menon G.K. (2002). New insights into skin structure: scratching the surface. Advanced Drug Delivery Reviews 54: S3-S17.

Meteyer C.U., Buckles E.L., Blehert D.S., Hicks A.C., Green D.E., Shearn-Bochsler V., Thomas N.J., Gargas A. & Behr M.J. (2009). Histopathologic criteria to confirm white-nose syndrome in bats. Journal of Veterinary Diagnostic Investigation 21: 411-414.

Meteyer C.U., Barber D. & Mandl J.N. (2012). Pathology in euthermic bats with white nose syndrome suggests a natural manifestation of immune reconstitution inflammatory syndrome. Virulence 3(7): 583-588.

Meyer J.M. & Abdallah M.A. (1978). The fluorescent pigment of *Pseudomonas fluorescens*: biosynthesis, purification and physiochemical properties. Journal of General Microbiology 107: 319-328.

Mühldorfer K., Speck S. & Wibbelt G. (2011). Diseases in free-ranging bats from Germany. BMC Veterinary Research 7: 61.

Mühldorfer K. (2013). Bats and bacterial pathogens: a review. Zoonoses and Public Health 60: 93-103.

Mulec J., Oarga-Mulec A., Šturm S., Tomazin R. & Matos T. (2017). Spacio-Temporal distribution and tourist impact on airborne bacteria in a cave (Škocjan Caves, Slovenia). Diversity 9: 28.

Peig J. & Green A.J. (2009) New perspectives for estimating body condition from mass/length data: the scaled mass index as an alternative method. Oikos 118: 1883-1891.

Peleg A.Y., Hogan D.A. & Mylonakis E. (2010) Medically important bacterial-fungal interactions. Nature Reviews Microbiology 8: 340-349.

Perniola R., Faneschi M.L., Manso E., Pizzolante M., Rizzo A., Damiani A.S. & Longo R. (2006). *Rhodotorula mucilaginosa* outbreak in neonatal intensive care unit: microbiological features, clinical presentation, and analysis of related variables. European Journal of Clinical Microbiology 25: 193-196.

Pfaller M.A., Diekema D.J. & Merz W.G. (2009). Infections caused by non-*Candida*, non-*Cryptococcus* yeasts. In: Anaissie E.J., McGinnis M.R., Pfaller M.A., editors. Clinical Mycology 2nd ed. New York: Churchill Livingstone Elsevier: 261p.

Phillips C.D., Phelan G., Dowd S.E., McDonough M.M., Ferguson A.W., Hanson J.D., Siles L., Ordóñez-Garza N., San Francisco M. & Baker R.J. (2012). Microbiome analysis among bats describes influences of host phylogeny, life history, physiology and geography. Molecular Ecology 21: 2617-2627.

Podschun R., Fischer A. & Ullmann U. (2001). Characterisation of *Hafnia alvei* isolates from human clinical extra-intestinal specimens: haemagglutinins, serum resistance and siderophore synthesis. Journal of Medical Microbiology 50: 208-214.

Powers K.E., Reynolds R.J., Orndoff W., Ford W.M. & Hobson C.S. (2015). Post-white-nose syndrome trends in Virginia's cave bats, 2008-2013. Journal of Ecology and the Natural Environment 7(4): 113-123.

Pulvirenti N., Dall'Oglio F., Greco A.M., Oliveri S., Schwartz R.A. & Micali G. (2006). Superficial cutaneous *Trichosporon asahii* infection in an immunocompetent host. International Journal of Dermatology 45: 1428-1431.

R Core Team (2018). R: A language and environment for statistical computing. R Foundation for Statistical Computing, Vienna, Austria. https://www.R-project.org/.

Real F., Fernández A., Acosta F., Acosta B., Castro P., Déniz S. & Orós J. (1997). Septicemia associated with *Hafnia alvei* in laying hens. Avian Diseases 41(3): 741-747.

Reeder D.M., Frank C.L., Turner G.G., Meteyer C.U., Kurta A., Britzke E.R., Vodzak M.E., Darling S.R., Stihler C.W., Hicks A.C., Jacob R., Grieneisen L.E., Brownlee S.A., Muller L.K. & Blehert D.S. (2012). Frequent arousal from hibernation linked to severity of infection and mortality in bats with white-nose syndrome. PLoS ONE 7(6): e38920.

Ringa, E. (2008). The ability of Carnobacteria isolated from fish intestine to inhibit growth of fish pathogenic bacteria: a screening study. Aquaculture Research 39: 171-180.

Robinson S., Milner-Gulland E.J., Grachev Y., Salemgareyev A., Orynbayev M., Lushchekina A., Morgan E., Beauvais W., Singh N., Khomenko S., Cammack R. & Kock R. (2019). Opportunistic bacteria and mass mortality in ungulates: lessons from an extreme event. Ecosphere 10(6): e02671.

Roth V.R., Arduino M.J., Nobiletti J., Holt S.C., Carson L.A., Wolf C.F.W., Lenes B.A., Allison P.M. & Jarvis W.R. (2000). Transfusion-related sepsis due to *Serratia liquefaciens* in the United States. Transfusion 40: 931-935.

Ryun K.H., Lee A.R., Kim J.H. & Ahn B.H. (2012). Microbial dynamics of commercial *Makgeolli* depending on the storage temperature. Journal of Microbiology and Biotechnology 22(8): 1101-1106.

Scales B.S., Dickson R.P. LiPuma J.L. & Huffnagle G.B. (2014). Microbiology, genomics, and clinical significance of the *Pseudomonas fluorescens* species complex, an unappreciated colonizer of humans. Clinical Microbiology Reviews 27(4): 927-948.

Schaffer P.A., Lifland B., Van Sommeran S., Casper D.R. & Davis C.R. (2012). Meningoencephalitis associated with *Carnobacterium maltaromaticum*-like bacteria in stranded juvenile salmon sharks (*Lamna ditropis*). Veterinary Pathology 50(3): 412-417.

Selvin J., Lanong S., Syiem D., De Mandal S., Kayang H., Kumar N.S. & Kiran G.S. (2019). Culture-dependent and metagenomic analysis of lesser horseshoe bats' gut

microbiome revealing unique bacterial diversity and signatures of potential human pathogens. Microbial Pathogenesis 137: 103675.

Sewall B.J., Scafini M.R. & Turner G.G. (2016). Prioritization and management of Pennsylvania's bat hibernacula after pervasive contamination with the fungus causing white-nose syndrome. In: Butchkoski, C.M., Reeder, D.M., Turner, G.G., Whidden, H.P., editors. Conservation and Ecology of Pennsylvania's Bats. East Stroudsburg, PA: Pennsylvania Academy of Science: 209p.

Shokohi T., Moradi N., Badram L., Badali H., Ataollahi M.R. & Afsarian M.H. (2018). Molecular identification of clinically common and uncommon yeast species. Jundishapur Journal of Microbiology 11(10): e66240.

Sugita T., Kikuchi K., Makimura K., Urata K., Someya T.., Kamei K., Niimi M. & Uehara Y. (2005). *Trichosporon* species isolated from guano samples obtained from bat-inhabited caves in Japan. Applied and Environmental Microbiology 71(11): 7626-7629.

Sun G. (2016). Mathematical modeling of population dynamics with Allee effect. Nonlinear Dynamics 85: 1–12.

Thammavongs B., Panoff J.M. & Guéguen M. (2000). Phenotypic adaptation to freeze-thaw stress of the yeast-like fungus *Geotrichum candidum*. International Journal of Food Microbiology. 60(1): 99-105.

Thogmartin W.E., King R.A., McKann P.C., Szymanski J.A. & Pruitt L. (2012). Population-level impact of white-nose syndrome on the endangered Indiana bat. Journal Of Mammalogy 93: 1086-1098.

Toljander J.F., Artursson V., Paul L.R., Jansson J.K. & Finlay R.D. (2006). Attachment of different soil bacteria to arbuscular mycorrhizal fungal extraradical hyphae is determined by hyphal vitality and fungal species. FEMS Microbiology Letters 254: 34-40.

Turner GG, Meteyer C, Barton H, Gumbs J, Reeder DM, B. Overton, Bandouchova H, Bartonička T, Martínková N, Pikula J, Zukal J & Blehert D. (2014). Non-lethal screening of bat wing skin using UV fluorescence to detect lesions indicative of white-nose syndrome. Journal Wildlife Diseases 50: 566-573.

USFWS. (2012). North American bat death toll exceeds 5.5 million from white-nose syndrome. 17 January, 2012. United States Fish and Wildlife Service, Arlington, VA. Available from https://www.whitenosesyndrome.org/press-release/north-american-bat-death-tool-exceeds-5-5-million-from-white-nose-syndrome

USFWS. (2018). National White-Nose Syndrome Decontamination Protocol - Version 09.13.2018. United States Fish and Wildlife Service. Available from www.whitenosesyndrome.org/topics/decontamination.

Van den Beld M.J.C., Reinders E., Notermans D.W. & Reubsaet F.A.G. (2016). Possible misidentification of species in the *Pseudomonas fluorescens* lineage as *Burkholderia pseudomallei* and *Francisella tularensis*, and emended descriptions of *Pseudomonas brenneri*, *Pseudomonas gessardii* and *Pseudomonas proteolytica*. International Journal of Systematic and Evolutionary Microbiology 66: 3420-3425.

Vanderwolf K.J., McAlpine D.F., Malloch D. & Forbes G.J. (2013). Ectomycota associated with hibernating bats in eastern Canadian caves prior to the emergence of white-nose syndrome. Northeastern Naturalist 20(1): 115-130.

Vengust M., Knapic T. & Weese J.S. (2018). The fecal bacterial microbiota of bats; Slovenia. PLoS ONE 13(5): e0196728.

Verant M.L., Meteyer C.U., Speakman J.R., Cryan P.M., Lorch J.M. & Blehert D.S. (2014). White-nose syndrome initiates a cascade of physiologic disturbances in the hibernating bat host. BMC Physiology 14: 10.

Voigt C.C., Caspers B. & Speck S. (2005). Bats, bacteria and bat smell: sex-specific diversity of microbes in a sexually selected scent organ. Journal of Mammalogy, 86(4): 745-749.

Voyron S., Lazzari A., Riccucci M., Calvini M., Varese G.C. (2011). First mycological investigation on Italian bats. Hystrix, the Italian Journal of Mammalogy 22(1): 189-197.

Walther G., Pawlowska J., Alastruey-Izquierdo A., Wrzosek M., Rodriguez-Tudela J.L., Dolatabadi S., Chakrabarti A. & de Hoog G.S. (2013). DNA barcoding in *Mucorales*: an inventory of biodiversity. Persoonia 30: 11-47.

Ward C.G., Clarkson J.G., Taplin D. & Polk Jr. H.C. (1967). Wood's light fluorescence and *Pseudomonas* burn wound infection. Journal of the American Medical Association 202(11): 127-128.

Warnecke L., Turner J.M., Bollinger T.K., Lorch J.M., Misra V., Cryan P.M., Wibbelt G., Blehert D.S. & Willis C.K.R. (2012). Inoculation of bats with European *Geomyces destructans* supports the novel pathogen hypothesis for the origin of white-nose syndrome. PNAS 109(18): 6999-7003.

Wasserman A.E. (1965). Absorption and fluorescence of water-soluble pigments produced by four species of *Pseudomonas*. Applied Microbiology 13(2): 175-180.

White T.J., Bruns T., Lee S. & Taylor J. (1990). Amplification and direct sequencing of fungal ribosomal RNA genes for phylogenetics. In: Innis M.A., Gelfand D.H., Sninsky J.J., White T.J., editors. PCR Protocols: A Guide to Methods and Applications. San Diego, CA: Academic Press: 315-322.

Wirth F. & Goldani L.Z. (2012). Epidemiology of *Rhodotorula*: an emerging pathogen. Interdisciplinary Perspectives on Infectious Disease 2012: 465717.

WNS Response Team (2020). White-Nose Response Team, United States Fish and Wildlife Service. Accessed from www.whitenosesyndrome.org .

Zenowiak D.J., Harrison T.P. & Caire W. (1993). External bacteria of hibernating *Myotis velifer* (Chiroptera: Vespertilionidae). The Southwestern Naturalist 38(1): 73-76.

Zhang T., Victor T.R., Rajkumar S.S., Li X., Okoniewski J.C., Hicks A.C., Davis A.D., Broussard K., LaDeau S.L., Chaturvedi S., Chaturvedi V. (2014). Mycobiome of the bat white nose syndrome affected caves and mines reveals diversity of fungi and local adaptation by the fungal pathogen *Pseudogymnoascus* (*Geomyces*) *destructans*. PLoS ONE 9(9): e108714.

APPENDIX A

Supplementary Methods

A1. Capture site and experimental site descriptions

All bats used in this study were captured from a maternity colony located in a suburban area of Huntingdon County, Pennsylvania. The maternity colony was inside one set of seven adjacent multi-chamber bat boxes (built by Bat Conservation & Management and the Pennsylvania Game Commission), positioned on top of 3.05-m-high wooden posts. The colony included 845 bats as of July of 2015, though at the time of capture, most bats using the site as a day roost had dispersed, possibly to travel to hibernation sites. The maternity colony was monitored in the weeks leading up to the capture effort. By the capture date on October 2, 2019, most bats had departed the site, but a few remained.

The abandoned iron mine used as the experimental site was closed to human visitation by bat-friendly gating. Rooms near the mine's entrance that maintained a relatively stable, cold temperature during winter were utilized for placement of cages. Four, double-layered wire mesh cages were bolted to the mine wall to house the bats in semi-natural conditions. A 1.5-inch x 0.75-inch lumber was used to create a wooden frame covered on five sides in wire mesh. The cages were open on the wall side to provide access to the wall substrate. The front of each cage, internal and external, was placed on a hinge to allow access to the bats during the study, and sliding locks were used to secure them when closed. Each cage was bolted to the wall at a height of approximately 1.5m to limit access by predators. The internal cage was 20.3 cm in height

and width, and 11.4 cm in depth, providing enough room for bats to cluster or roost separately, and to move around the cage during arousal events. The external cage was 45.7 cm in height and width and 24.1 cm deep, providing a 12.7 cm buffer all around the internal cage to prevent predation events. A small gravity-fed water trough was provided to the bats throughout hibernation, supplied by a 20-oz water bottle attached on the outside of the internal cage. Expanding insulation foam was used to fill any gaps between the wooden cages and the mine walls, and a roof was made out of cedar plank for each cage to prevent moisture dripping directly onto the hibernating bats.

Sediment containing *Pd* was applied to the cage and wall substrates one week prior to the installation of the bats. Spores were cultured from a local Pennsylvania strain of *Pd* and equilibrated to a concentration of 500 *Pd* spores/mL using dilution techniques and a hemocytometer. Sediment from a mine environment was autoclaved twice for 60 minutes, then separated into four 10 g aliquots. The sediment sections were individually placed on sterile petri dishes. Each sterile sediment sample was inoculated with 1 mL spore solution using a pipettor, yielding sediment samples with identical concentrations of *Pd*. These sediment samples were spread gently across areas that could be accessed by bats within each of the four cages, including the mine wall and the inside of the cage. This procedure enabled us to ensure *Pd* was present and in standardized amounts within the areas that could be accessed by bats in their cages.

A2. Bat capture procedure

To reduce impact on the little brown myotis population, only male bats were captured and the effort was focused on an area of the state with a relatively large population of the species. Additionally, to reduce the likelihood *Pd* would be present on

bats at capture, effort was focused on the period just prior to entry into hibernation (which begins in October in the area) rather than after the onset of hibernation. I targeted male little brown myotis for use in this study. The juvenile males captured were those late to leave the maternity colony for hibernation, and the adult males were presumably visiting the maternity colony to mate with females. At the maternity colony in fall, adult males visited in early evening, a situation that enabled us to capture adult and juvenile male little brown myotis at a single site just prior to hibernation. Little brown myotis males were captured at evening emergence on October 2, 2018, with three 1.8 m by 2.3 m harp traps set one meter off the ground in front of the bat box containing the maternity colony. A total of 10 juvenile male and 9 adult male little brown myotis were captured.

A3. Data collection

For each bat, forearm length was measured using calipers with a precision of ± 0.01 mm, and mass was taken on a digital scale with precision of ± 0.01 g (Ohaus Valor 3000 Xtreme). Uniquely-numbered lightweight aluminum bands were applied to each bat's right forearm. Evaluation of the presence or extent of WNS infection was completed by trans-illuminating each wing with long-wave (368 nm) ultraviolet light (using a Way Too Cool light box) and photographed with a Canon Rebel D digital camera with a 100 mm macro EF lens. The camera was mounted on a tripod with 65 cm between the wing and the end of the lens, on manual mode with 2-second shutter speed, f/5.6, and ISO 100. A new set of nitrile gloves was used for each individual bat and each was placed into a new paper bag to avoid cross-contamination of bats with *Pd*.

A4. Transport to experimental site

Following capture, bats were individually enclosed in moistened cloth bags and hung in a DC-powered portable refrigeration unit (Dometic Ltd., Bedfordview, South Africa) set to 4°C. High humidity levels were maintained within the unit via evaporation from sponges saturated with water. The cold and humid conditions mimicked conditions within the hibernation site to trigger torpor expression, and minimize energy loss and evaporative water loss during transport. The bats were relocated to the experimental site the same night as capture.

A5. Post-mortem examination and culturing

In the post-mortem examinations of the deceased little brown myotis, one frequently examined adult was vivisected using a sterilized scalpel to examine organs. Skin, liver, heart and kidney tissues were macerated in 1% sterile peptone buffer using a high speed centrifuge. 1 mL of each sample was plated onto both Acidified Rose Bengal Agar (ARBA) and Tryptic Soy Agar (TSA) mediums. ARBA inhibits the growth of bacteria and supports the growth of yeasts and molds. TSA is complementary to the ARBA as it encourages bacterial growth. Additional tissue samples from the macerated liver, heart, lung and kidney were placed in 1% sterile peptone buffer and incubated at 32˚C for 48 hours. After incubation, 1 mL of each solution was plated onto both ARBA and TSA mediums. Liquid-filled vesicles in the wing membrane were separated using fungal tape and examined under a light microscope. The vesicles were then sonicated in 1% peptone buffer and 1 ml was plated on TSA and ARBA mediums. The plates were incubated at 9˚C – 10˚C for 10 days before morphotypes for both fungal and bacterial colonies were determined, and colony counts were made. Bacteria and fungi were

differentiated using colony morphology and counts on plates, and cell morphology observed through light microscopy, as well as gram staining results for bacteria. Individual morphotypes were isolated, and sub-cultured on a series of plates to obtain pure cultures for sequencing.

I plated 13 wing swabs, taken from living bats before termination of the experiment. These swabs were streaked directly on to both TSA and ARBA plates to analyze each bat's external microbiome and mycobiome before death. The plates were incubated at 9˚C – 10˚C for 12 days before morphotypes were determined and colony counts were made. Colonies of interest were then isolated and streaked on individual plates. TSA medium was used for bacterial colonies, and ARBA was used for fungi. Slides were created of the isolated species, and they were examined under a light microscope. The plates were incubated at 9˚C – 10˚C for 16 days and colonies of interest were isolated, and plated on TSA medium if bacterial, and RBA medium if fungal. After another 14 day incubation period, bacterial isolates were gram-stained and slides were made of all cultures. Using gram-staining results, colony morphology, and cell morphology from observation under a light microscope, unique organisms were identified for sequencing.

A6. DNA extraction and amplification

To amplify the isolates' DNA for sequencing, 50 µL of Elution Buffer was added to individual centrifuge tubes for each culture. Using a heat sterilized loop, one bacterial colony or a scraping of fungal mycelium was added to its respective tube. For the bacterial PCR, nine samples were then placed in the PCR Thermocycler at 95˚C for five minutes to denature the DNA. Bacterial gene primers 17F (GTTTGATCCTGGCTCAG)

and 1492R (GGTTACCTTGTTACGACTT) were used to anneal 1400 base pairs of the 16S ribosomal RNA gene. A master mix consisting of 275µL of Dream TAQ®, 5.5 µL 17F, 5.5 µL 1429R, and 242 µL water was created in a 1.5 mL centrifuge tube and then vortexed to combine. To each of nine new sample centrifuge tubes and one control tube, 48 µL of the master mix was added (25 µL of Dream TAQ®, 0.5 µL of each primer, and 22 µL of water in each tube) and the tubes were vortexed. Afterward, 2 µL of denatured DNA from each isolate was added to one of the nine sample tubes, leaving the control without DNA. The 10 tubes were then placed into the PCR Thermocycler, which cycled through temperatures 95˚ C for 1 minute, 55˚ C for 1 minute, and 72˚ C for 1 minute for a total of 3 hours. This process allowed the DNA to denature, the primers to anneal and the PCR product to elongate. The bacterial PCR products were refrigerated overnight before sequencing. For the fungal PCR, 3 tubes containing 50 µL of Elution Buffer and a fungal mycelium scraping from one of the 3 isolates were placed into the PCR Thermocycler at 95˚C for 10 minutes to denature the DNA. Fungal primers ITS1 (TCCGTAGGTGAACCTGCGG) and ITS4 (TCCTCCGCTTATTGATATGC) were used to amplify the internal transcribed spacer region of fungal DNA. These primers are commonly used to amplify the ITS region – a region with higher variability than other genic regions of fungal rDNA, making species-level identification possible (White et al. 1990). A master mix consisting of 125µL of Dream TAQ®, 2.5 µL ITS1, 2.5 µL ITS4, and 110 µL water was created in a 1.5 mL centrifuge tube and then vortexed to combine. To each of 3 new sample centrifuge tubes and one control tube, 48 µL of the master mix was added and the tubes were vortexed. Afterward, 2 µL of denatured DNA from each isolate was added to one of the 3 sample tubes, leaving the control without DNA. The 4

tubes were then placed into the PCR Thermocycler, which cycled through temperatures 95˚ C for 1 minute, 55˚ C for 1 minute, and 72˚ C for 1 minute for a total of 3 hours. Afterward the samples were stored in 10˚C cold storage prior to sequencing.

To check the success of amplification, PCR products were visualized using gel electrophoresis. To prepare the gel, 0.3 g of Agarose and 30mL of TAE Buffer were combined and microwaved for 45 seconds, and 2 µL of SYBR stain was added to the heated mixture. The solution was then poured into a gel electrophoresis plate with combs placed to create wells, and the gel was allowed to cool for 30 minutes. After cool, the gel was covered with water and the combs were removed. For the bacterial samples, 10 µL from each of the 9 samples and one control was added to individual wells in the gel. For the fungal samples, 10 µL of each of the 3 samples and 1 control was added to individual wells. Cables were attached and the gels were run at 140 volts for 18 minutes. The gels were photographed under UV illumination to determine presence of PCR product.

The successful PCR products were then cleaned using the ChargeSwitch®-Pro PCR Clean-up Kit following Centrifugation Protocol (Invitrogen, Carlsbad, CA, USA). Cleaned PCR products of the isolated fungi and bacteria were then frozen and shipped to Penn State Core Facility (State College, Pennsylvania) for bidirectional DNA sequencing using the forward and reverse primers.

APPENDIX B

Supplementary Tables

Age	Monitoring Category	Total	Capture		Week 2		Week 4		Week 7	
			BMI / SMI	Wing Damage	BMI / SMI	Wing Damage	BMI / SMI	Wing Damage	BMI / SMI	Wing Damage
Juvenile	Frequently-Examined	5	5	5	5	5	4	2	n/a	n/a
Adult	Frequently-Examined	5	5	5	5	5	5	4	2	2
Juvenile	Less-Examined	5	5	5	n/a	n/a	5	2	n/a	n/a
Adult	Less-Examined	4	4	4	n/a	n/a	n/a	n/a	1	1

Table B1. Sample sizes throughout the experiment Sample sizes decreased throughout the experiment due to increasing mortality and a premature end to the study for juveniles at week 4.

	Frequently Examined										Less Disturbed									
	Juvenile					Adult					Juvenile					Adult				
	61134	*61135*	*61140*	*61145*	*61148*	*60024*	*61131*	*61132*	*61139*	*61143*	*61133*	*61136*	*61138*	*61142*	*61146*	*61137*	*61144*	*61147*	*61149*
Capture	0.00%	0.00%	0.00%	0.00%	0.06%	0.00%	0.00%	0.00%	0.00%	0.00%	0.00%	0.00%	0.00%	0.00%	0.00%	0.00%	0.00%	0.00%	0.00%
Week 2	0.00%	0.00%	0.00%	0.00%	0.02%	0.00%	0.00%	0.00%	0.00%	0.00%										
Week 4 *Juvenile End*		0.01%		0.01%		0.00%	0.00%		0.00%	0.00%		0.02%	0.00%							
Week 7 *Adult End*						0.01%				0.03%						0.09%				

Table B2. Percent wing area infected by *Pd* throughout experiment Fluorescence representative of cupping erosions from *Pd* never exceeded 0.1% of the total area of both the left and right wings of the little brown myotis in the experiment.